Matsuda, K., Sakamoto, H., Kawata, M., 2008. Androgen action in the brain and spinal cord for the regulation of male sexual behaviors. Curr. Opin. Pharmacol. 8, 747–751.

Molnar, Z., Vasistha, N.A., Garcia-Moreno, F., 2011. Hanging by the tail: progenitor populations proliferate. Nat. Neurosci. 14, 538–540.

Nagao, T., Wada, K., Kuwagata, M., Nakagomi, M., Watanabe, C., Yoshimura, S., Saito, Y., Usumi, K., Kanno, J., 2004. Intrauterine position and postnatal growth in Sprague-Dawley rats and ICR mice. Reprod. Toxicol. 18, 109–120.

Nakamura, K., Itoh, K., Sugimoto, T., Fushiki, S., 2007. Prenatal exposure to bisphenol A affects adult murine neocortical structure. Neurosci. Lett. 420, 100–105.

Nakamura, K., Itoh, K., Yaoi, T., Fujiwara, Y., Sugimoto, T., Fushiki, S., 2006. Murine neocortical histogenesis is perturbed by prenatal exposure to low doses of bisphenol A. J. Neurosci. Res. 84, 1197–1205.

Noctor, S.C., Martinez-Cerdeno, V., Ivic, L., Kriegstein, A.R., 2004. Cortical neurons arise in symmetric and asymmetric division zones and migrate through specific phases. Nat. Neurosci. 7, 136–144.

Pulgar, R., Olea-Serrano, M.F., Novillo-Fertrell, A., Rivas, A., Pazos, P., Pedraza, V., Navajas, J.M., Olea, N., 2000. Determination of bisphenol A and related aromatic compounds released from bis-GMA-based composites and sealants by high performance liquid chromatography. Environ. Health Perspect. 108, 21–27.

Sasaki, N., Okuda, K., Kato, T., Kakishima, H., Okuma, H., Abe, K., Tachino, H., Tuchida, K., Kubono, K., 2005. Salivary bisphenol-A levels detected by ELISA after restoration with composite resin. J. Mater. Sci. Mater. Med. 16, 297–300.

Schonfelder, G., Wittfoht, W., Hopp, H., Talsness, C.E., Paul, M., Chahoud, I., 2002. Parent bisphenol A accumulation in the human maternal-fetal-placental unit. Environ. Health Perspect. 110, A703–A707.

Takayanagi, S., Tokunaga, T., Liu, X., Okada, H., Matsushima, A., Shimohigashi, Y., 2006. Endocrine disruptor bisphenol A strongly binds to human estrogen-related receptor gamma (ERRgamma) with high constitutive activity. Toxicol. Lett. 167, 95–105.

Wang, L., Andersson, S., Warner, M., Gustafsson, J.A., 2003. Estrogen receptor (ER)beta knockout mice reveal a role for ERbeta in migration of cortical neurons in the developing brain. Proc. Natl. Acad. Sci. U. S. A. 100, 703–708.

Xu, L.C., Sun, H., Chen, J.F., Bian, Q., Qian, J., Song, L., Wang, X.R., 2005. Evaluation of androgen receptor transcriptional activities of bisphenol A, octylphenol and nonylphenol in vitro. Toxicology 216, 197–203.

Ye, X., Kuklenyik, Z., Needham, L.L., Calafat, A.M., 2005. Quantification of urinary conjugates of bisphenol A, 2,5-dichlorophenol, and 2-hydroxy-4-methoxybenzophenone in humans by online solid phase extraction-high performance liquid chromatography-tandem mass spectrometry. Anal. Bioanal. Chem. 383, 638–644.

Yoshida, M., Shimomoto, T., Katashima, S., Watanabe, G., Taya, K., Maekawa, A., 2004. Maternal exposure to low doses of bisphenol a has no effects on development of female reproductive tract and uterine carcinogenesis in Donryu rats. J. Reprod. Dev. 50, 349–360.

Zsarnovszky, A., Belcher, S.M., 2001. Identification of a developmental gradient of estrogen receptor expression and cellular localization in the developing and adult female rat primary somatosensory cortex. Brain Res. Dev. Brain Res. 129, 39–46.

The American Journal of Pathology, Vol. 180, No. 1, January 2012

DOI: 10.1016/j.ajpath.2011.09.027

Immunopathology and Infectious Diseases

CCR7 with $S1P_1$ Signaling through AP-1 for Migration of $Foxp3^+$ Regulatory T-Cells Controls Autoimmune Exocrinopathy

Naozumi Ishimaru,* Akiko Yamada,* Takeshi Nitta,† Rieko Arakaki,* Martin Lipp,‡ Yousuke Takahama,† and Yoshio Hayashi*

From the Department of Oral Molecular Pathology, Institute of Health Biosciences, The University of Tokushima Graduate School, Tokushima, Japan; the Department of Experimental Immunology,† Institute for Genome Research, The University of Tokushima, Tokushima, Japan; and the Department of Molecular Tumor Genetics and Immunogenetics,‡ Max-Delbruck Center for Molecular Medicine, Berlin, Germany*

Forkhead box p3-positive ($Foxp3^+$) regulatory T cells (T_{reg} cells) participate in maintaining peripheral immune tolerance and suppressing autoimmunity. We recently reported that *in situ* patrolling by C-C-chemokine receptor 7 $(CCR7)^+$ T_{reg} cells in target organs is essential for controlling autoimmune lesions in Sjögren's syndrome. In the present study, the molecular mechanism underlying CCR7-mediated T_{reg} cell migration was investigated in a mouse model. The impaired migratory response of $Ccr7^{-/-}$ T_{reg} cells to sphingosine 1-phosphate (S1P) occurred because of defective association of S1P receptor 1 ($S1P_1$) with a G coupled–protein. In addition, T-cell receptor (TCR)- and $S1P_1$-mediated Ras-related C3 botulinum toxin substrate 1 (Rac-1), extracellular signal-related kinase (ERK), and c-Jun phosphorylation required for activator protein 1 (AP-1) transcriptional activity were significantly impaired in $Ccr7^{-/-}$ T_{reg} cells. Surprisingly, the abnormal nuclear localization of Foxp3 was detected after abrogation of the c-Jun and Foxp3 interaction in the nucleus of $Ccr7^{-/-}$ T_{reg} cells. These results indicate that CCR7 essentially controls the migratory function of T_{reg} cells through $S1P_1$-mediated AP-1 signaling, which is regulated through its interaction with Foxp3 in the nucleus. *(Am J Pathol 2012, 180: 199–208; DOI: 10.1016/j.ajpath.2011.09.027)*

Regulatory T cells (T_{reg} cells) are a unique subset of T cells that play a critical role in maintaining immune tolerance.[1–3] The expression of the transcription factor forkhead box p3 (Foxp3) is the genetic hallmark of T_{reg} cells.[4–6] Foxp3-targeted genes in T_{reg} cells are up-regulated or down-regulated, suggesting that Foxp3 functions as both a transcriptional activator and a repressor.[7] Previous evidence indicates that Foxp3 controls T_{reg} functions by interacting with multiple transcription factors.[8] The function or expression of Foxp3 is controlled through complexes formed with other transcription factors, such as nuclear factor of activated T cells (NFAT), RUNX1/acute myelogenous leukemia (AML) 1, and nuclear factor kappa-B (NF-κB).[9,10] In addition, Foxp3 can maintain T_{reg} cell unresponsiveness (anergy) by selectively inhibiting the promoter DNA-binding activity of activator protein 1 (AP-1).[11] However, the molecular mechanism by which Foxp3 switches between transcriptional activation and repression in T_{reg} cells has not been well defined.

Previously, we reported autoimmune exocrinopathy in salivary and lacrimal glands resembling Sjögren's syndrome in C-C-chemokine receptor 7 (CCR7)-deficient ($Ccr7^{-/-}$) mice.[12] Enhanced immunity in $Ccr7^{-/-}$ mice is caused by defective lymph node (LN) positioning of T_{reg} cells and consequent impairment of suppressor function.[13] In a recent report, we demonstrated that CCR7 essentially governs the patrolling functions of T_{reg} cells by controlling their migration to target organs to maintain autoimmunity.[14] Furthermore, we found that the migratory function of $Ccr7^{-/-}$ T_{reg} cells in response to sphingosine 1-phosphate (S1P) was impaired, suggesting that CCR7

Supported by Funding Program for Next Generation World-Leading Researchers in Japan (LS090), Grants-in-Aid for Scientific Research (no. 17109016 and 17689049) from the Ministry of Education, Science, Sport, and Culture of Japan, and by funds from the Uehara Memorial Foundation and the Takeda Science Foundation (N.I.).

Accepted for publication September 13, 2011.

Supplemental material for this article can be found at *http://ajp.amjpathol.org* or at doi: 10.1016/j.ajpath.2011.09.027.

Address reprint requests to Naozumi Ishimaru, D.D.S., Ph.D., Department of Oral Molecular Pathology, Institute of Health Biosciences, The University of Tokushima Graduate School, 3-18-15 Kuramotocho, Tokushima 770-8504, Japan. E-mail: ishimaru@dent.tokusghima-u.ac.jp.

participates in the molecular mechanism underlying the migratory function of peripheral T_{reg} cells through S1P and one of its receptors, $S1P_1$.[14] In contrast, at the molecular level, T_{reg} cells in $S1P_1$-deficient mice were found to be defective in egress from the thymus; the number of peripheral T_{reg} cells in $S1P_1$-deficient mice was also increased, compared with peripheral T_{reg} cells in control mice.[15] Furthermore, $S1P_1$ transgenic mice developed autoimmune lesions because of a decrease in the number of T_{reg} cells in the thymus.[15] The S1P-$S1P_1$ axis is thus believed to play an important role in restraining the development and function of $Foxp3^+$ T_{reg} cells.

Mitogen-activated protein kinase (MAPK) signaling and AP-1 components are crucial in $S1P_1$ signaling in peripheral T cells.[16] In addition, the function of T_{reg} cells can be regulated by Foxp3 binding to phosphorylated c-Jun, thereby controlling AP-1 transcriptional activity.[11] Although the relationship between CCR7 and S1P/$S1P_1$ signaling in peripheral T_{reg} cells has not been clarified, it is possible that interactions among several molecules (including CCR7, S1P/$S1P_1$, and Foxp3) play a critical role in controlling the migratory response of peripheral T_{reg} cells.

In the present study, analysis of defective T_{reg} cells in *Ccr7*$^{-/-}$ mice revealed a novel regulation of Foxp3 nuclear localization that controls $S1P_1$-mediated AP-1 signaling after T_{reg} cell migration.

Materials and Methods

Mice

Ccr7$^{-/-}$, *Ccr7*$^{+/+}$ and C57BL/6 mice were reared in our specific pathogen-free mouse colony. Mice were provided food and water *ad libitum*. Experiments were humanely conducted under the regulation and permission of the Animal Care and Use Committee of the University of Tokushima (Tokushima, Japan).

Histological Analysis

All organs were removed from mice, fixed with 10% phosphate-buffered formaldehyde (pH 7.2), and prepared for histological examination. Sections were stained with H&E.

Cell Preparation

T_{reg} cells and $CD25^-CD4^+$ cells were enriched from LNs. In brief, $CD4^+$ cells were prepared using anti-B220, CD8, MHC class II, and NK1.1 monoclonal antibodies (mAbs) (eBioscience, San Diego, CA) and magnetic beads (Dynal Biotech, Oslo, Norway). $CD25^+CD4^+$ or $CD25^-CD4^+$ cells were enriched using biotin-conjugated anti-CD25 mAb, magnetic beads, and a CELLection biotin binder kit (Dynal Biotech) or a regulatory T cell isolation kit (Miltenyi Biotec, Auburn, CA). The enriched $CD25^+CD4^+$ cells were confirmed to be approximately 90% $Foxp3^+$.

In Vitro *Suppression Assay*

For suppression assays, a total of 5×10^4 $CD25^-CD4^+$ T cells from C57BL/6 mice were stimulated with plate-coated anti-CD3 mAb (0.5 μg/mL) for 72 hours together with 1.25, 2.5, and 5×10^4 $CD25^+CD4^+$ T cells from the LNs of wild-type (WT) and *Ccr7*$^{-/-}$ mice. [^{3}H]-Thymidine incorporation during the last 12 hours of the culture for 72 hours was evaluated using an automated liquid scintillation β counter (Hitachi Aloka Medical, Ltd., Tokyo, Japan).

ELISA

For detection of IL-4, IL-10, and TGF-β, $CD25^+CD4^+$ T cells were stimulated with plate-coated anti-CD3 mAb for 24 hours. The supernatants were added to microtiter plates precoated with an antibody specific for IL-4, IL-10, and TGF-β. The biotinylated antibody was added, and the plate was incubated for 2 hours at room temperature. After a wash, streptavidin-horseradish peroxidase solution was added to each well and the plate was incubated for 30 minutes. Finally, stabilized chromogen substrate was added to each well, and the absorbance of each well was read at 450 nm using an automated microplate reader (Bio-Rad Laboratories, Hercules, CA). Cytokine concentrations were obtained according to standard curves.

Confocal Microscopic Analysis

Cells were deposited onto poly-L-lysine-coated glass slides, and spun in a cytospin centrifuge. Sections were stained with 1 μg/mL of primary antibodies against phosphorylated ERK1/2, phosphorylated c-Jun (BD Biosciences, San Jose, CA), phosphorylated Rac-1 (Cell Signaling Technology, Danvers, MA), and Foxp3 (eBioscience, San Diego, CA) for 1 hour. After three washes in PBS, sections were stained with Alexa Fluor 568 donkey anti-rat IgG (H+L) (Molecular Probes; Invitrogen, Carlsbad, CA) or Alexa Fluor 488 horse anti-rabbit IgG (H+L) secondary antibodies for 30 minutes and washed with PBS. The nuclei were stained with DAPI. Sections were visualized with a laser scanning confocal microscope (Carl Zeiss MicroImaging, Göttingen, Germany). A 63×/1.4 oil differential interference contrast (DIC) objective lens was used. Quick Operation software, version 3.2 (Carl Zeiss), was used for image acquisition and Adobe Photoshop CS2 software (Adobe System, San Jose, CA) was used for image processing. Nuclear localization of Foxp3 and DAPI was evaluated within the imaging system.

Real-Time Quantitative RT-PCR

Total RNA was extracted from the T_{reg} cells of WT and *Ccr7*$^{-/-}$ mice with ISOGEN (Wako Pure Chemical, Osaka, Japan) and was then reverse-transcribed. Transcript levels of Gi, Rac-1, Foxp3, and β-actin were analyzed using the DNA engine OPTICOM system (Bio-Rad Laboratories) with SYBR Premix Ex Tag (Takara, Kyoto,

Japan). Primer sequences were as follows: Gi forward, 5′-TTTCTCTGGATGGGATGAGG-3′ and reverse, 5′-CCGAACCTCATGTTGTGTTG-3′; Rac-1 forward, 5′-GCCACTCAACGAGAGCCTAC-3′ and reverse, 5′-TCGGTTCTCCAGCTTGACTT-3′; Foxp3 forward, 5′-CCCAGGAAAGACAGCAACCTT-3′ and reverse, 5′-TTCTCACAACCAGGCCACTTG-3′; and β-actin forward, 5′-AAATCTGGCACCACACCTTC-3′ and reverse, 5′-GAGGCGTACAGGGATAGCA-3′.

Cell Culture and Migration Assay

For cell culturing with S1P or chemokines, cells were incubated in RPMI 1640 medium without fetal calf serum in the presence of S1P (0 to 100 nmol/L), CCL19 (100 ng/mL), or CCL21 (100 ng/mL) with plate-coated anti-CD3 mAb (0.5 μg/mL) for 3 to 12 hours. To evaluate chemotaxis by S1P, CCL19, or CCL21 in the T_{reg} cells of WT and *Ccr7*$^{-/-}$ mice, a Cultrex 96-well cell migration assay kit (Trevigen, Gaithersburg, MD) was used according to the manufacturer's instructions. Before the assay, the cells were starved for 24 hours in serum-free medium and incubated in RPMI 1640 without fetal calf serum. In addition, the cells were pretreated with inhibitors, including FTY720 (BioVision, San Francisco, CA), PTX, rapamycin, SB203580, and PD98059 (Sigma-Aldrich, St. Louis, MO) for 6 to 12 hours, and then the migration assay was performed.

Western Blotting and Immunoprecipitation

Whole-cell extracts of T_{reg} cells were prepared using a Pierce M-PER mammalian protein extraction kit (Thermo Fisher Scientific, Rockford, IL) or nuclear/cytosol fraction kit (BioVision). A total of 10 μg of each sample per well was applied to each well and was electrophoresed on 10% SDS-PAGE. Thereafter, the protein was electrophoretically transferred onto polyvinylidene difluoride membranes. Blocked membranes were incubated with antibodies specific for $S1P_1$ (Cayman Chemical, Ann Arbor, MI), Rac-1, phosphorylated Rac-1 (Cell Signaling Technology), Gi (Millipore-Chemicon International, Temecula, CA), phospho-c-Jun (BD Biosciences), total c-Jun (BD Biosciences), or glyceraldehyde-3-phosphate dehydrogenase (GAPDH; Santa Cruz Biotechnology, Santa Cruz, CA). Horseradish peroxidase-conjugated rabbit or mouse IgG was used as the secondary antibody. Protein binding was visualized using Amersham ECL Western blotting detection reagents (GE Healthcare, Piscataway, NJ). To quantify protein expression, the chemiluminescence image was analyzed using a ChemiDoc XRS system (Bio-Rad Laboratories). For immunoprecipitation, purified proteins captured with anti-Foxp3 mAb were incubated with Dynabeads protein G (Invitrogen). To remove genomic DNA, proteins were treated with DNase I. Precipitated proteins were analyzed by immunoblotting with anti-c-Jun or anti-Foxp3 (e-Bioscience) antibody.

c-Jun Transcriptional Activity

The transcriptional activity of c-Jun in the nuclear extracts from T_{reg} of WT and *Ccr7*$^{-/-}$ mice was analyzed using an Upstate c-Jun transcription factor assay kit (Millipore, Billerica, MA). In brief, nuclear extracts were incubated with a biotinylated double-stranded oligonucleotide probe containing the consensus sequence for c-Jun on a streptavidin-coated plate. Captured complexes were incubated with c-Jun antibody, horseradish peroxidase-conjugated secondary antibody, and tetramethylbenzidine substrate. The absorbance of samples was measured using an automated microplate reader at 450 nm.

Statistical Analysis

Student's *t*-test was used for statistical analysis. A P value of <0.05 was considered statistically significant.

Results

Relationship between Autoimmune Lesions and T_{reg} Cells in Ccr7$^{-/-}$ Mice

We found a significantly reduced proportion of Foxp3$^+$ T_{reg} cells in target organs, including the salivary and lacrimal glands, of *Ccr7*$^{-/-}$ mice, compared with *Ccr7*$^{+/+}$ mice, at approximately 3 months of age. This led to significantly increased retention of T_{reg} cells in the LNs of *Ccr7*$^{-/-}$ mice until mice were 6 months of age.[14] However, it is unclear whether the proportion of T_{reg} cells in target organs and LNs changed with aging during these 6 months. More severe autoimmune lesions in lacrimal glands of *Ccr7*$^{-/-}$ mice were observed at 9 and 18 months of age (Figure 1A). At 18 months of age, extensive infiltration of lymphocytes with destruction of exocrine gland cells was detected in *Ccr7*$^{-/-}$ mice (Figure 1A). The proportion of Foxp3$^+$ CD4$^+$ T_{reg} cells in the cervical LNs of *Ccr7*$^{-/-}$ mice was significantly increased, compared with WT mice, until 18 months of age (Figure 1B). The retention of T_{reg} cells in the LNs of *Ccr7*$^{-/-}$ mice increased with aging. In contrast, the proportion of T_{reg} cells in lacrimal glands of *Ccr7*$^{-/-}$ mice was significantly reduced, compared with *Ccr7*$^{+/+}$ mice (Figure 1C). In addition, although the absolute number of T_{reg} cells in the cervical LNs of normal mice decreased with aging, the number of LN T_{reg} cells in *Ccr7*$^{-/-}$ mice increased (Figure 1D). At 3 and 9 months of age, the cell number in T_{reg} cells in *Ccr7*$^{-/-}$ mice was significantly reduced, compared with control mice (Figure 1D). At 18 months of age, the number of cells of *Ccr7*$^{-/-}$ mice was similar to that of control mice (Figure 1D). Given that the total cell number in the LNs of *Ccr7*$^{-/-}$ mice significantly decreased, compared with control mice, the proportion of T_{reg} cells from *Ccr7*$^{-/-}$ mice was higher than that from control mice (Figure 1B). In contrast, the number of T_{reg} cells in lacrimal glands of *Ccr7*$^{-/-}$ mice were significantly reduced, compared with control mice (Figure 1E). These findings are consistent with our previous report that Foxp3$^+$ CD4$^+$

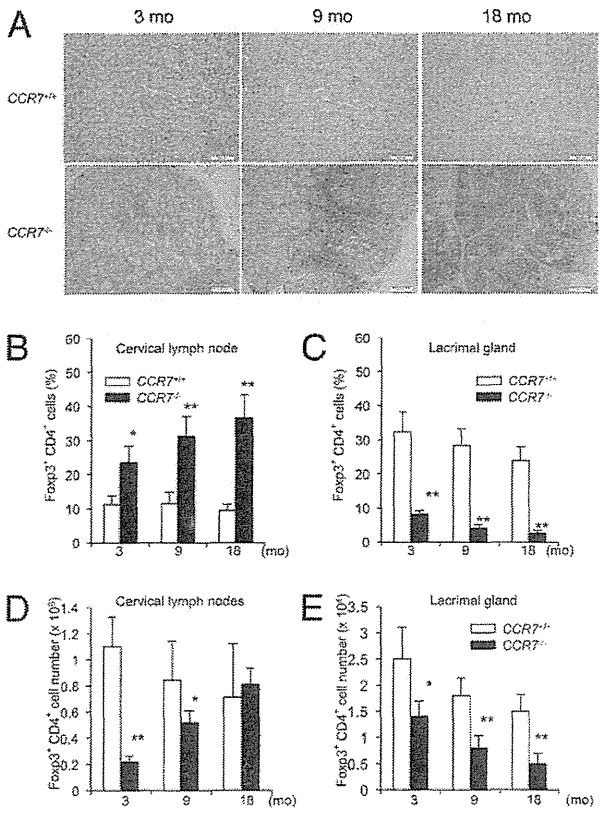

Figure 1. Autoimmune exocrinopathy and T_{reg} cell in *Ccr7*$^{-/-}$ mice. **A:** Histology of lacrimal glands of *Ccr7*$^{+/+}$ and *Ccr7*$^{-/-}$ mice at 3, 9, and 18 months of age. H&E staining was performed on paraffin-embedded sections. Images are representative of 5 to 7 mice per group. Scale bars = 500 μm. **B:** The proportions of Foxp3$^+$ CD4$^+$ T_{reg} cells in cervical LNs in *Ccr7*$^{+/+}$ and *Ccr7*$^{-/-}$ mice at 3, 9, and 18 months of age were detected by flow cytometric analysis. **C:** The proportions of Foxp3$^+$ CD4$^+$ T_{reg} cells in lacrimal glands of *Ccr7*$^{+/+}$ and *Ccr7*$^{-/-}$ mice at 3, 9, and 18 months of age were detected by flow cytometric analysis. **D:** Quantification of Foxp3$^+$ CD4$^+$ T_{reg} cells in cervical LNs of *Ccr7*$^{+/+}$ and *Ccr7*$^{-/-}$ mice at 3, 9, and 18 months of age. **E:** Quantification of Foxp3$^+$ CD4$^+$ T_{reg} cells in lacrimal glands of *Ccr7*$^{+/+}$ and *Ccr7*$^{-/-}$ mice at 3, 9, and 18 months of age. Results are presented as means ± SD for five mice in each group. $^*P < 0.05$; $^{**}P < 0.005$ versus WT.

T_{reg} cell numbers are significantly reduced in target organs, such as salivary or lacrimal glands, in *Ccr7*$^{-/-}$ mice and in patients with Sjögren's syndrome.[14]

Chemotactic Response to S1P and Suppressive Function of Ccr7$^{-/-}$ T_{reg} *Cells*

We examined in *vitro* chemotactic responses of CD4$^+$ T cells from WT and *Ccr7*$^{-/-}$ mice in response to S1P. In both WT and *Ccr7*$^{-/-}$ mice, no migratory responses of CD25$^+$CD4$^+$ T_{reg} cells were observed with the addition of S1P (Figure 2A). Although there was a small increase in the chemotactic response of WT and *Ccr7*$^{-/-}$ CD25$^-$CD4$^+$ T cells to S1P, there were no differences in the response between WT and *Ccr7*$^{-/-}$ mice (Figure 2B). Next, we examined the chemotactic response of anti-CD3 mAb-engaged *Ccr7*$^{-/-}$ CD4$^+$ cells to S1P, and found that the migratory response of *Ccr7*$^{-/-}$ T_{reg} cells to S1P was significantly impaired, compared with WT T_{reg} cells (Figure 2C). In contrast, the response of CD25$^-$CD4$^+$ cells of *Ccr7*$^{-/-}$ mice was not impaired (Figure 2D). These findings suggest that the chemotactic response of T cells to S1P is dependent on T-cell receptor/CD3 signaling.

To determine whether there were migratory responses to chemoattractants other than S1P, we performed migration assays using IL-6 and MIP-2, and found no difference in the migration activity between WT and *CCR7*$^{-/-}$ T_{reg} cells. The results for anti-CD3 mAb-engaged T_{reg} cells are shown in Figure 2, E and F. Moreover, there were also no differences in migration activity in response to IL-6 and MIP-2 between unstimulated WT and *CCR7*$^{-/-}$ T_{reg} cells (data not shown). In contrast, when we examined the *in vitro* suppressive function of *Ccr7*$^{-/-}$ T_{reg} cells, we found that the suppression of *Ccr7*$^{-/-}$ T_{reg} cells on the proliferative response elicited by the anti-CD3 mAb in normal CD25$^-$CD4$^+$ cells from C57BL/6 mice was similar to that of WT T_{reg} cells (Figure 2G). In addition, there were no differences in the production of suppressive cytokines such as IL-4, IL-10, or TGF-β in *Ccr7*$^{-/-}$ or WT T_{reg} cells (Figure 2H). These findings suggest that CCR7 signaling controls the migration of T_{reg} cells, but does not control the suppressive function of T_{reg} cells. This is consistent with the failure of *in vivo* migration to target organs in *Ccr7*$^{-/-}$ T_{reg} cells.[14]

Activation of Signaling Molecules Downstream of $S1P_1$ *in* Ccr7$^{-/-}$ T_{reg} *Cells*

$S1P_1$, one of receptors for S1P, is expressed on the cell surface and is known to be internalized when the S1P ligand binds to $S1P_1$ after activation of the signaling molecules required for the migratory response.[17] We detected expression of $S1P_1$ in WT and *Ccr7*$^{-/-}$ T_{reg} cells by Western blotting with anti-$S1P_1$ polyclonal antibodies. There was no difference in $S1P_1$ expression between WT and *Ccr7*$^{-/-}$ T_{reg} cells (Figure 3, A and B). $S1P_1$ has been shown to signal exclusively through the heterotrimeric G protein Gi.[18] We therefore used Western blotting to evaluate Gi expression in WT and *Ccr7*$^{-/-}$ T_{reg} cells after anti-CD3 mAb and S1P treatment (see Supplemental Figure S1A at *http://ajp.amjpathol.org*). There were no differences in expression between WT and *Ccr7*$^{-/-}$ T_{reg} cells, and this was unchanged by stimulus (see Supplemental Figure S1A at *http://ajp.amjpathol.org*).

The phosphorylation of Rac-1,[19] a key molecule downstream of G-protein signaling, was observed in WT T_{reg} cells but not in *Ccr7*$^{-/-}$ T_{reg} cells stimulated with the anti-CD3 mAb and S1P (Figure 3C). Phosphorylation of Rac-1 was evaluated by Western blotting. The phosphorylation of Rac-1 in WT T_{reg} cells was detectable after CD3 engagement, and the addition of S1P enhanced Rac-1 phosphorylation in anti-CD3 mAb-stimulated T_{reg} cells (Figure 3D). In contrast, the phosphorylation of Rac-1 in *Ccr7*$^{-/-}$ T_{reg} cells was low, compared with that in WT T_{reg} cells (Figure 3D). In contrast, there was no difference in Rac-1 phosphorylation between WT and *Ccr7*$^{-/-}$ CD25$^-$CD4$^+$ T cells (see Supplemental Figure S2 at *http://ajp.amjpathol.org*). These findings demonstrate the impairment of the signaling pathway in *Ccr7*$^{-/-}$ T_{reg} cells.

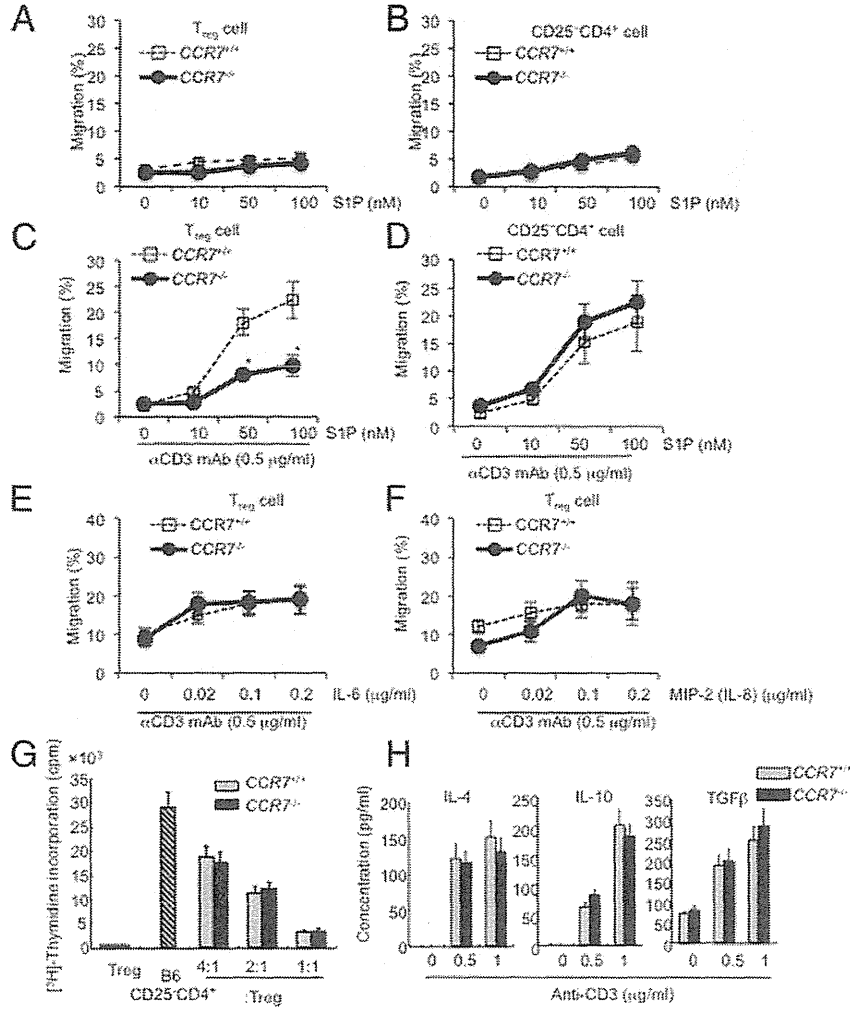

Figure 2. Signaling pathway in *Ccr7*$^{-/-}$ T_{reg} cells. **A** and **B:** Migration assay of T_{reg} cells (**A**) and $CD25^-CD4^+$ T cells (**B**) from LNs of WT and *Ccr7*$^{-/-}$ mice in response to S1P (0 to 100 nmol/L) was performed using purified T_{reg} and $CD25^-CD4^+$ T cells for 12 hours. **C** and **D:** Migration assay of T_{reg} cells (**C**) and $CD25^-CD4^+$ T cells (**D**) from LNs of WT and *Ccr7*$^{-/-}$ mice in response to S1P (0 to 100 nmol/L) was performed using anti-CD3mAb-stimulated T cells for 12 hours. **E:** Migratory response to IL-6 (0 to 0.2 μg/mL) in anti-CD3 mAb-stimulated T_{reg} cells. **F:** Migratory response to MIP-2 (0 to 0.2 μg/mL) in anti-CD3 mAb-stimulated T_{reg} cells. Data are presented as means ± SD (n = 3) and are representative of three independent experiments. **G:** *In vitro* suppression assays were performed by evaluation of the proliferative response in purified $CD25^-CD4^+$ T cells from C57BL/6 mice. $CD25^-CD4^+$ T cells were cocultured with WT or *Ccr7*$^{-/-}$ T_{reg} cells on anti-CD3 mAb-coated plates for 72 hours. The proliferative response was evaluated by incorporation of [^{3}H]-thymidine during the last 18 hours of incubation. Data are presented as means ± SD (n = 3) and are representative of three independent experiments. **H:** WT or *Ccr7*$^{-/-}$ T_{reg} cells were stimulated with anti-CD3 mAb for 24 hours. Concentrations of IL-4, IL-10, and TGF-β in the culture supernatants were measured by enzyme-linked immunosorbent assay. Data are presented as means ± SD (n = 3) and are representative of two independent experiments.

Next, we focused on examining migratory function and CCR7 signaling using a Gi protein inhibitor, pertussis toxin (PTX), and an S1P receptor agonist, FTY720 (Figure 3E). The increased migratory response of WT T_{reg} cells on stimulation with anti-CD3 mAb and S1P was reduced by pretreatment with FTY720 or PTX (Figure 3E). Moreover, when WT T_{reg} cells were incubated with a CCR7 ligand (either CCL19 or CCL21) in addition to anti-CD3 mAb and S1P, migratory responses were significantly enhanced in contrast to the response to anti-CD3 mAb and S1P (Figure 3E). These enhanced responses were reduced with pretreatment of FTY720 and PTX to the levels of *Ccr7*$^{-/-}$ T_{reg} cells (Figure 3E). This result suggests that CCR7 signaling in T_{reg} cells is dependent on cooperation with S1P/$S1P_1$ and Gi, in addition to CD3 signaling.

MAPK Signaling in Ccr7$^{-/-}$ T_{reg} *Cells*

To further elucidate the importance of $S1P_1$ signaling for T_{reg} cell egress, we analyzed MAPK signaling and the AP-1 components that play crucial roles in $S1P_1$ signaling in T cells.[16] Phosphorylation of ERK after stimulation with anti-CD3 mAb and S1P was observed in WT T_{reg} cells, but not in *Ccr7*$^{-/-}$ T_{reg} cells (Figure 4A), and this phosphorylation was enhanced with addition of S1P (Figure 4B). To determine whether this signaling was through MAPK or Akt-mTOR, we performed migration assays using the mTOR inhibitor rapamycin and two MAPK inhibitors. The migratory activity of WT T_{reg} cells increased with treatment of anti-CD3 mAb and S1P, and was not fully inhibited by pretreatment with rapamycin (Figure 4C). The increased migratory response of WT T_{reg} cells was significantly inhibited by the addition of the ERK MAPK inhibitor PD98059, but not by the addition of the p38 MAPK inhibitor SB203580 (Figure 4C). These findings suggest that CCR7-mediated ERK activation plays a crucial role in the migratory function of T_{reg} cells.

Association of c-Jun Activity with CCR7/$S1P_1$ *Signaling*

When T_{reg} cells of WT mice were stimulated with anti-CD3 mAb and S1P, phosphorylated c-Jun protein colocalized with Foxp3 in the nucleus. In contrast, phosphorylation of c-Jun was undetectable in *Ccr7*$^{-/-}$ T_{reg} cells stimulated

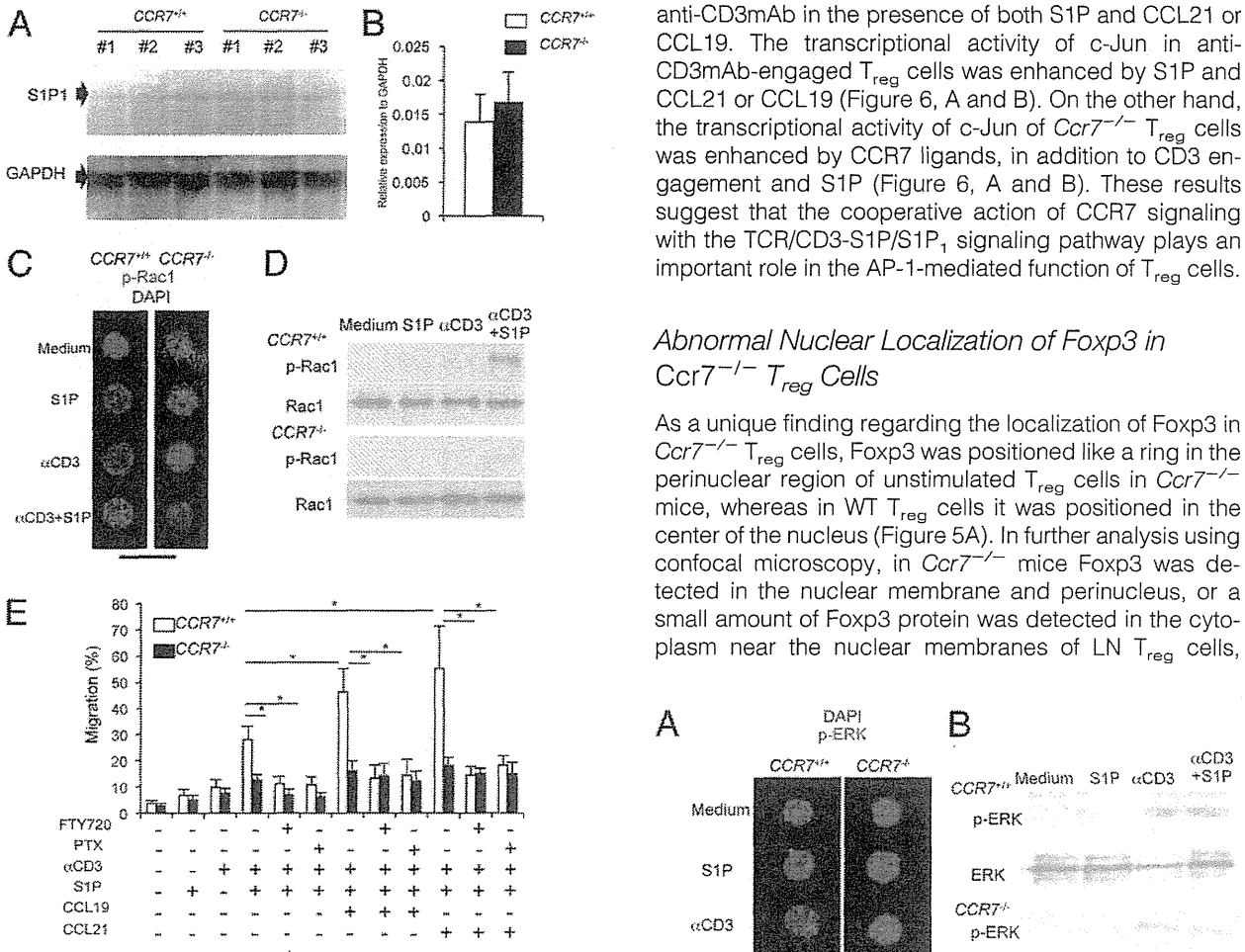

Figure 3. $S1P_1$ expression in $Ccr7^{-/-}$ T_{reg} cells. **A:** Western blotting of $S1P_1$ in T_{reg} cells from WT and $Ccr7^{-/-}$ mice (n = 3/group) was performed. GAPDH expression was used as a housekeeping protein. **B:** Relative expression of $S1P_1$ to GAPDH was quantified using the protein band intensities in A. Data are presented as means ± SD (n = 3). **C:** Phosphorylation of Rac-1 in T_{reg} cells of LNs from WT and $Ccr7^{-/-}$ mice was analyzed under confocal microscopy. Nuclei were stained with DAPI. Images are representative of three mice in each group. Scale bar =10 μm. **D:** Western blot analysis of Rac-1 and phosphorylated Rac-1 was performed. Results are representative of three independent experiments. **E:** Migration assay of WT and $Ccr7^{-/-}$ T_{reg} cells was performed using anti-CD3 mAb (0.5 mg/mL), S1P (100 nmol/L), CCL19 (50 ng/mL), CCL21 (50 ng/mL), and pretreatment (6 hours) with FTY720 or PTX. Data are presented as means ± SD (n = 3) and are representative of three independent experiments. $^*P < 0.05$.

with anti-CD3 mAb in the presence of S1P (Figure 5A). In support of these findings, the immunoblot analysis showed much stronger phosphorylation of c-Jun in WT T_{reg} cells stimulated with anti-CD3 mAb and S1P than in $Ccr7^{-/-}$ T_{reg} cells (Figure 5B). Furthermore, the transcriptional activity of c-Jun was significantly increased using nuclear extracts from WT T_{reg} cells stimulated with anti-CD3 mAb and S1P, compared with extracts from $Ccr7^{-/-}$ T_{reg} cells (Figure 5C). These results show that the CCR7-dependent TCR/CD3-S1P/$S1P_1$ signaling pathway is critical for T_{reg} function through AP-1 activation.

To examine whether the transcriptional activity of c-Jun is controlled by CCR7 ligands (CCL21 and CCL19), we analyzed the activity of WT T_{reg} cells stimulated with anti-CD3mAb in the presence of both S1P and CCL21 or CCL19. The transcriptional activity of c-Jun in anti-CD3mAb-engaged T_{reg} cells was enhanced by S1P and CCL21 or CCL19 (Figure 6, A and B). On the other hand, the transcriptional activity of c-Jun of $Ccr7^{-/-}$ T_{reg} cells was enhanced by CCR7 ligands, in addition to CD3 engagement and S1P (Figure 6, A and B). These results suggest that the cooperative action of CCR7 signaling with the TCR/CD3-S1P/$S1P_1$ signaling pathway plays an important role in the AP-1-mediated function of T_{reg} cells.

Abnormal Nuclear Localization of Foxp3 in Ccr7$^{-/-}$ T_{reg} Cells

As a unique finding regarding the localization of Foxp3 in $Ccr7^{-/-}$ T_{reg} cells, Foxp3 was positioned like a ring in the perinuclear region of unstimulated T_{reg} cells in $Ccr7^{-/-}$ mice, whereas in WT T_{reg} cells it was positioned in the center of the nucleus (Figure 5A). In further analysis using confocal microscopy, in $Ccr7^{-/-}$ mice Foxp3 was detected in the nuclear membrane and perinucleus, or a small amount of Foxp3 protein was detected in the cytoplasm near the nuclear membranes of LN T_{reg} cells,

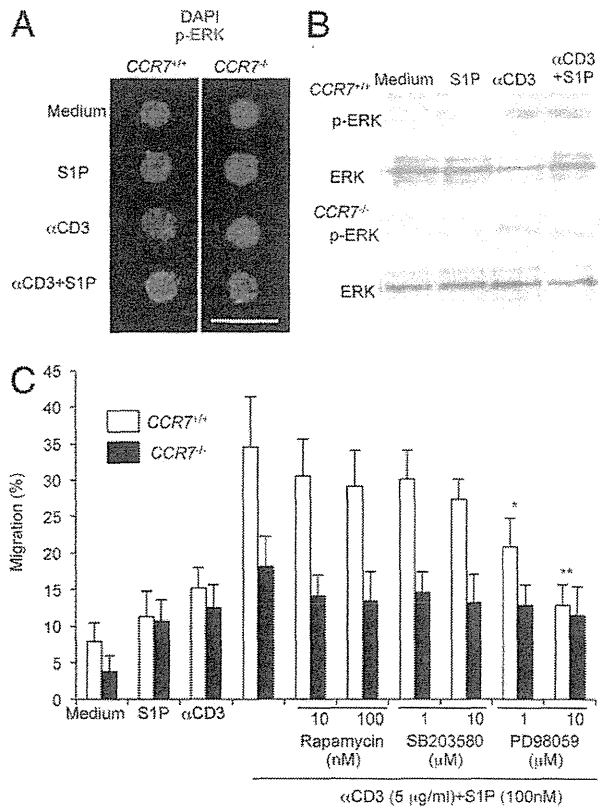

Figure 4. Signaling pathway downstream of $S1P_1$ in $Ccr7^{-/-}$ T_{reg} cells. **A:** Phosphorylation of ERK in $Foxp3^+$ T_{reg} cells of LNs from WT and $Ccr7^{-/-}$ mice was detected under confocal microscopy. Scale bar = 10 μm. **B:** Phosphorylation of ERK and total ERK in $Foxp3^+$ T_{reg} cells of LNs from WT and $Ccr7^{-/-}$ mice were detected by Western blotting. **C:** Migration assay of WT and $Ccr7^{-/-}$ T_{reg} cells was performed using anti-CD3 mAb (0.5 mg/mL), S1P (100 nmol/L), CCL19 (50 ng/mL), CCL21 (50 ng/mL), and pretreatment (6 hours) with rapamycin (10 and 100 nmol/L), SB203580 (1 and 10 μmol/L), or PD98059 (1 and 10 μmol/L). Data are presented as means ± SD (n = 3) and are representative of three independent experiments. $^*P < 0.05$; $^{**}P < 0.005$.

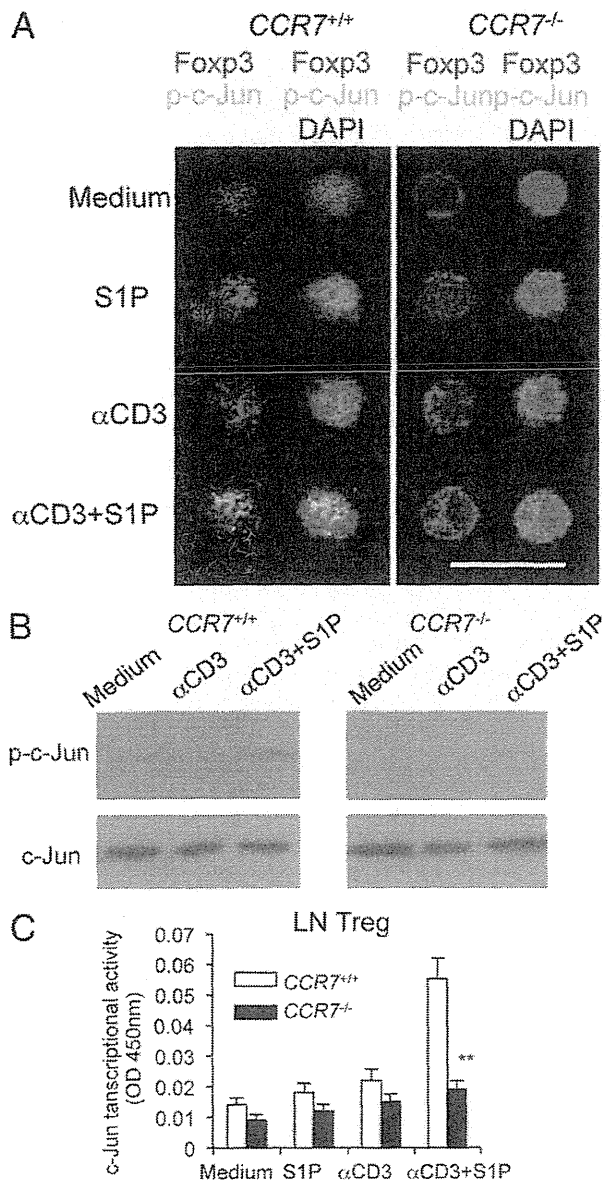

Figure 5. MAPK and AP-1 signaling in T_{reg} cells through $S1P_1$ and CCR7. **A:** Foxp3 and phospho-c-Jun in LN T_{reg} cells from WT and *Ccr7*$^{-/-}$ mice were analyzed under confocal microscopy. Nuclei were stained with DAPI. Results are representative of three independent experiments. Scale bar = 10 μm. **B:** Detection of phospho-c-Jun and total c-Jun in LN T_{reg} cells from WT and *Ccr7*$^{-/-}$ mice was analyzed by Western blot. Results are representative of two independent experiments. **C:** c-Jun transcriptional activity of LN T_{reg} cells from WT and *Ccr7*$^{-/-}$ mice was measured using an AP-1 binding probe. Data are presented as means ± SD (n = 3) and are representative of two independent experiments. $^{**}P < 0.005$ versus WT.

whereas in WT T_{reg} cells it was present exclusively in the nucleus (Figure 7, A and B). Even when *Ccr7*$^{-/-}$ T_{reg} cells were cultured without stimulus (medium only), Foxp3 was localized in the perinuclear region of the cell (Figure 5A,). When *Ccr7*$^{-/-}$ T_{reg} cells were stimulated with anti-CD3 mAb or anti-CD3 mAb + S1P, Foxp3 was localized both in the perinucleus and in the center of the nucleus (Figure 5A). These findings suggest that CCR7 regulates the nuclear localization of Foxp3. According to a recent report, Foxp3 significantly suppresses the transcriptional activity and promoter DNA binding of AP-1 by interacting with c-Jun, indicating that Foxp3 is a suppressor of c-Jun-based AP-1 transcriptional activity.[11] The binding of Foxp3 to c-Jun in WT T_{reg} cells stimulated by anti-CD3 mAb and S1P, was observed by immunoprecipitation with anti-Foxp3 mAb; however, this binding was not present in *Ccr7*$^{-/-}$ T_{reg} cells (Figure 7C). In contrast, there were no differences in mRNA expression of Foxp3 between WT and *Ccr7*$^{-/-}$ T_{reg} cells (Figure 7D). It is may be that Foxp3 is localized in the perinuclear region of the cells because of impaired c-Jun activation in *Ccr7*$^{-/-}$ T_{reg} cells.

Discussion

In the present study, we confirmed two possible molecular mechanisms underlying T_{reg} cell function mediated by CCR7. In one mechanism, our results suggest that the cooperative action of CCR7 with TCR/CD3 controls the internalization of $S1P/S1P_1$ with Gi after the phosphorylation of c-Jun as well as MAPK activation in T_{reg} cells (see Supplemental Figure S3 at *http://ajp.amjpathol.org*). The other mechanism shows that Foxp3 can bind to phosphorylated c-Jun in the nucleus to inhibit the transcriptional activity required for the migratory function or unresponsiveness of Treg cells. In contrast, c-Jun unbound from Foxp3 in the nucleus may act as a transcription factor for the migratory function of peripheral T_{reg} cells (see Supplemental Figure S3 at *http://ajp.amjpathol.org*). We hypothesize that the migratory function of T_{reg} cells is controlled by c-Jun activation, which is regulated by the $S1P/S1P_1$ pathway through the cooperative action between TCR/CD3 and CCR7 signaling and the molecular interaction of Foxp3 with c-Jun. In contrast, in *Ccr7*$^{-/-}$ T_{reg} cells, defective internalization of $S1P/S1P_1$ after ac-

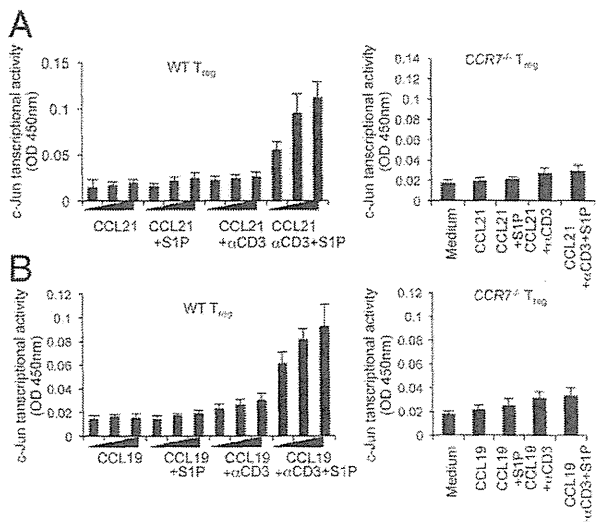

Figure 6. Control of c-Jun transcriptional activity in T_{reg} cells by ligation with CCR7. The c-Jun transcriptional activity of WT and *Ccr7*$^{-/-}$ T_{reg} cells stimulated with plate-coated anti-CD3mAb (0.5 μg/mL) in the presence of S1P and CCL21 (0, 20, 50 ng/mL) (**A**) or CCL19 (0, 20, 50 ng/mL) (**B**) was evaluated. For *Ccr7*$^{-/-}$ T_{reg} cells, CCL19 and CCL21 were used (50 ng/mL). Data are presented as means ± SD (n = 3) and are representative of two independent experiments. OD, optical density.

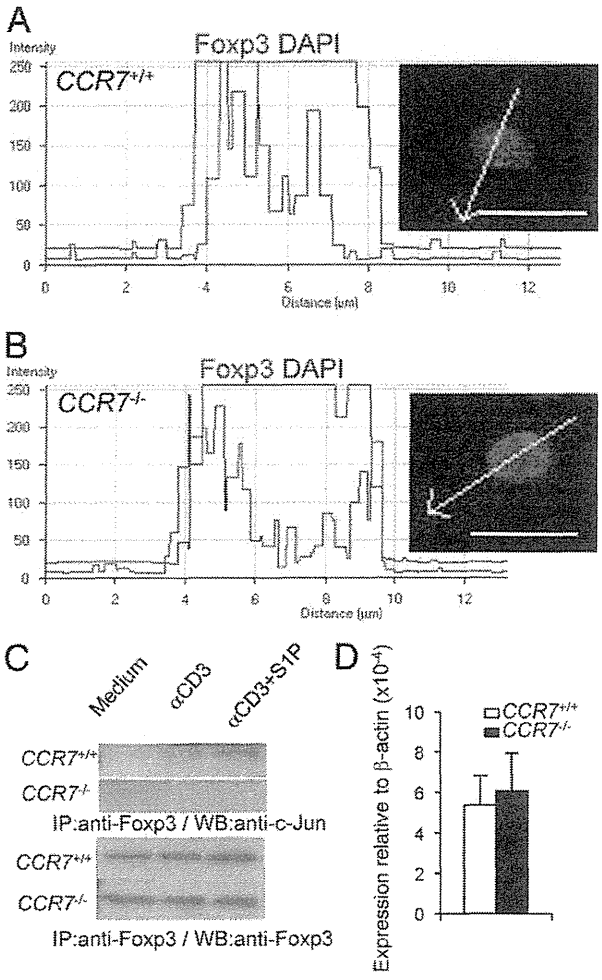

Figure 7. Abnormal nuclear localization of Foxp3 and impaired binding of Foxp3 to c-Jun. **A** and **B:** Nuclear localization of Foxp3 was evaluated by confocal microscopy analysis with DAPI staining. Relative fluorescence intensity of Foxp3 and DAPI along the axis of the arrow in the direction pointed by the arrow is shown. Results are representative of two independent experiments. Scale bars = 10 μm. **C:** Impairment of interaction between Foxp3 and c-Jun in *Ccr7*$^{-/-}$ T_{reg} was detected by immunoprecipitation with anti-Foxp3 mAb and by Western blotting with anti-c-Jun pAb. Results are representative of two independent experiments. **D:** Foxp3 mRNA expression was quantified by real-time PCR. Data are presented as means ± SD (n = 3).

tivation of MAPK and c-Jun may result in an impaired migratory response. It was reported that Foxp3 suppresses both the transcriptional activity and promoter DNA-binding of AP-1 by interacting with c-Jun, and this is related to the unresponsiveness of T_{reg} cells.[11] Our findings suggest that CCR7/S1P$_1$ signaling through the interaction of c-Jun and Foxp3 in T_{reg} cells controls migratory functions, in addition to the unresponsiveness of T_{reg} function. This may explain the defective *in vivo* function of *Ccr7*$^{-/-}$ T_{reg} cells.

S1P is one of the natural lysophospholipids that control various functions of immune cells, such as migration, proliferation, and cytokine secretion.[20–23] S1P is secreted by macrophages, mast cells, dendritic cells, and platelets.[24,25] The concentration of S1P is higher in the blood and lymph (range, 0.1 to 3 μmol/L) than in the lymphoid organs and other tissues (range, 3 to 100 nmol/L).[26,27] The S1P concentration gradient in each organ or tissue can control the chemotactic emigration of thymocytes and egress of lymphocytes from LNs during the differentiation or activation of certain pathological conditions.[28,29] More importantly, the condition of cell surface expression of S1P receptors regulates immune cell functions such as egress from LNs.[30,31] Among the five S1P G protein-coupled receptors (ie, S1P$_1$ though S1P$_5$), S1P$_1$ is the major S1P receptor responsible for the direct chemotactic response in T cells.[32–34] S1P$_1$ expressed on the T-cell surface is internalized when T cells are activated through the binding of S1P-S1P$_1$.[17] In the present study, although total expression of S1P$_1$ in *Ccr7*$^{-/-}$ T_{reg} cells was not significantly changed compared with that in WT T_{reg} cells, migratory function of WT T_{reg} cells in the response to CD3 signaling and S1P was impaired by treatment with a Gi inhibitor. In addition, CCR7 ligand-enhanced migratory response of WT T_{reg} cells was also inhibited by treatment with a Gi inhibitor. This finding suggests that CCR7 controls S1P/S1P$_1$-mediated T_{reg}-specific functions through CD3 signaling. However, the precise mechanism underlying CCR7 and S1P$_1$ signaling remains to be clarified.

TCR/CD3-dependent stimulation of T cells induces the down-regulation of plasma membrane S1P$_1$,[17] and activation of several molecules downstream of S1P$_1$ including Rac-1, ERK, and c-Jun, after AP-1 activation plays a critical role in S1P/S1P$_1$-mediated T cell functions.[15,35] Our results show that the activation of signaling molecules in MAPK and AP-1 pathways through TCR/CD3 and S1P$_1$ in *Ccr7*$^{-/-}$ T_{reg} cells was abrogated. In addition, CD3/S1P-induced transcriptional activity of c-Jun in normal Treg cells was enhanced by the addition of a CCR7 ligand (CCL21 or CCL19). This result suggests that the possible crosstalk between CCR7 and S1P/S1P$_1$ signaling plays an important role in TCR/CD3-mediated activation or peripheral T_{reg} cell migration. A recent report indicates that S1P$_1$ delivers an intrinsic negative signal to restrain thymic generation, peripheral maintenance, and suppressive activity of T_{reg} cells.[36] Furthermore, it was demonstrated that S1P$_1$ induces the selective activation of the Akt-mTOR kinase pathway to impede the development and function of T_{reg} cells.[15] Although the present study was focused on the migratory function of peripheral T_{reg} cells and not the development and function of thymic T_{reg} cells, we note that the Akt-mTOR pathway may be associated with the S1P$_1$-AP-1 pathway. Because the phosphorylation of ERK in *Ccr7*$^{-/-}$ T_{reg} cells was abrogated by stimulation with anti-CD3 mAb and S1P, but ERK activation in WT T_{reg} cells was detectable, it is possible that the Akt-mTOR pathway can act at any step in the S1P$_1$-AP-1 pathway. Our results show that ERK activation through CCR7/CD3/S1P$_1$ signaling is more crucial than Akt-mTOR for the migratory functions of T_{reg} cells. Further analysis of the molecular interactions between various signaling molecules is warranted.

Foxp3 plays an essential role in suppressing AP-1 DNA-binding activity and consequently inhibiting AP-1 transcription activity, because the expression of Foxp3 significantly blocked AP-1 transcriptional activity and promoter DNA binding.[11] A previous report suggested

that the blocking of AP-1 transcriptional activity by Foxp3 is associated with the unresponsiveness of T_{reg} cells because of inhibition of AP-1-mediated activation of T_{reg} cells.[11] In addition, transcriptional activation of c-Jun is inhibited in anergic T cells.[37–39] In the present study, signaling after AP-1 activation of *Ccr7*$^{-/-}$ T_{reg} cells was impaired. As a result, binding of Foxp3 to c-Jun in the nucleus was also undetectable in *Ccr7*$^{-/-}$ T_{reg} cells. The unresponsiveness of T_{reg} cells through the abrogated activation of c-Jun may be related to *in vivo* defects in the function of *Ccr7*$^{-/-}$ T_{reg} cells, as we have previously reported.[14] Mutations within a putative nuclear localization signal near the C-terminal end of the forkhead domain in the Foxp3 gene abrogate nuclear import of the Foxp3 protein.[40] Although the specific abnormality in the Foxp3 gene of *Ccr7*$^{-/-}$ mice is unclear, the impaired signaling of c-Jun by binding Foxp3 in *Ccr7*$^{-/-}$ T_{reg} cells may influence the localization of the Foxp3 protein. However, it is still unclear whether differentiation in the thymus or maturation in the periphery causes abnormal localization of Foxp3 in the nucleus of *Ccr7*$^{-/-}$ T_{reg} cells.

In summary, the present data show that CCR7 signaling can control the migratory response of T_{reg} cells through a possible crosstalk between Foxp3 and the S1P/$S1P_1$-AP-1 pathway. The characterization of this molecular mechanism is important in defining the pathogenesis of autoimmunity based on defects in T_{reg} cellular function.

Acknowledgments

We thank Satoko Katada, Ai Katayama, and Noriko Kino for their technical assistance and Kensuke Takada for the *in vivo* experiments.

References

1. Sakaguchi S: Naturally arising CD4+ regulatory T cells for immunologic self-tolerance and negative control of immune responses. Annu Rev Immunol 2004, 22:531–562
2. Sakaguchi S, Yamaguchi T, Nomura T, Ono M: Regulatory T cells and immune tolerance. Cell 2008, 133:775–787
3. Zheng Y, Rudensky AY: Foxp3 in control of the regulatory T cell lineage. Nat Immunol 2007, 8:457–462
4. Hori S, Nomura T, Sakaguchi S: Control of regulatory T cell development by the transcription factor Foxp3. Science 2003, 299:1057–1061
5. Sakaguchi S, Ono M, Setoguchi R, Yagi H, Hori S, Fehervari Z, Shimizu J, Takahashi T, Nomura T: Foxp3+ CD25+ CD4+ natural regulatory T cells in dominant self-tolerance and autoimmune disease. Immunol Rev 2006, 212:8–27
6. Wan YY, Flavell RA: Regulatory T-cell functions are subverted and converted owing to attenuated Foxp3 expression. Nature 2007, 445: 766–770
7. Zheng Y, Josefowicz SZ, Kas A, Chu TT, Gavin MA, Rudensky AY: Genome-wide analysis of Foxp3 target genes in developing and mature regulatory T cells. Nature 2007, 445:936–940
8. Li B, Saouaf SJ, Samanta A, Shen Y, Hancock WW, Greene MI: Biochemistry and therapeutic implications of mechanisms involved in FOXP3 activity in immune suppression. Curr Opin Immunol 2007, 19:583–588
9. Ono M, Yaguchi H, Ohkura N, Kitabayashi I, Nagamura Y, Nomura T, Miyachi Y, Tsukada T, Sakaguchi S: Foxp3 controls regulatory T-cell function by interacting with AML1/Runx1. Nature 2007, 446: 685–689
10. Wu Y, Borde M, Heissmeyer V, Feuerer M, Lapan AD, Stroud JC, Bates DL, Guo L, Han A, Ziegler SF, Mathis D, Benoist C, Chen L, Rao A: FOXP3 controls regulatory T cell function through cooperation with NFAT. Cell 2006, 126:375–387
11. Lee SM, Gao B, Fang D: FoxP3 maintains Treg unresponsiveness by selectively inhibiting the promoter DNA-binding activity of AP-1. Blood 2008, 111:3599–3606
12. Kurobe H, Liu C, Ueno T, Saito F, Ohigashi I, Seach N, Arakaki R, Hayashi Y, Kitagawa T, Lipp M, Boyd RL, Takahama Y: CCR7-dependent cortex-to-medulla migration of positively selected thymocytes is essential for establishing central tolerance. Immunity 2006, 24:165–177
13. Schneider MA, Meingassner JG, Lipp M, Moore HD, Rot A: CCR7 is required for the in vivo function of CD4+ CD25+ regulatory T cells. J Exp Med 2007, 204:735–745
14. Ishimaru N, Nitta T, Arakaki R, Yamada A, Lipp M, Takahama Y, Hayashi Y: In situ patrolling of regulatory T cells is essential for protecting autoimmune exocrinopathy. PLoS One 2010, 5:e8588
15. Liu G, Burns S, Huang G, Boyd K, Proia RL, Flavell RA, Chi H: The receptor S1P1 overrides regulatory T cell-mediated immune suppression through Akt-mTOR. Nat Immunol 2009, 10:769–777
16. Liao JJ, Huang MC, Graler M, Huang Y, Qiu H, Goetzl EJ: Distinctive T cell-suppressive signals from nuclearized type 1 sphingosine 1-phosphate G protein-coupled receptors. J Biol Chem 2007, 282: 1964–1972
17. Rivera J, Proia RL, Olivera A: The alliance of sphingosine-1-phosphate and its receptors in immunity. Nat Rev Immunol 2008, 8:753–763
18. Means CK, Miyamoto S, Chun J, Brown JH: S1P1 receptor localization confers selectivity for Gi-mediated cAMP and contractile responses. J Biol Chem 2008, 283:11954–11963
19. Matsuyuki H, Maeda Y, Yano K, Sugahara K, Chiba K, Kohno T, Igarashi Y: Involvement of sphingosine 1-phosphate (S1P) receptor type 1 and type 4 in migratory response of mouse T cells toward S1P. Cell Mol Immunol 2006, 3:429–437
20. Goetzl EJ, Rosen H: Regulation of immunity by lysosphingolipids and their G protein-coupled receptors. J Clin Invest 2004, 114: 1531–1537
21. Goetzl EJ, Wang W, McGiffert C, Huang MC, Gräler MH: Sphingosine 1-phosphate and its G protein-coupled receptors constitute a multifunctional immunoregulatory system. J Biol Chem 2004, 92:1104–1114
22. Graeler M, Goetzl EJ: Activation-regulated expression and chemotactic function of sphingosine 1-phosphate receptors in mouse splenic T cells. FASEB J 2002, 16:1874–1878
23. Graeler M, Shankar G, Goetzl EJ: Cutting edge: suppression of T cell chemotaxis by sphingosine 1-phosphate. J Immunol 2002, 169: 4084–4087
24. Olivera A, Rivera J: Sphingolipids and the balancing of immune cell function: lessons from the mast cell. J Immunol 2005, 174: 1153–1158
25. Pappu R, Schwab SR, Cornelissen I, Pereira JP, Regard JB, Xu Y, Camerer E, Zheng YW, Huang Y, Cyster JG, Coughlin SR: Promotion of lymphocyte egress into blood and lymph by distinct sources of sphingosine-1-phosphate. Science 2007, 316:295–298
26. Lee MJ, Van Brocklyn JR, Thangada S, Liu CH, Hand AR, Menzeleev R, Spiegel S, Hla T: Sphingosine-1-phosphate as a ligand for the G protein-coupled receptor EDG-1. Science 1998, 279:1552–1555
27. Schwab SR, Pereira JP, Matloubian M, Xu Y, Huang Y, Cyster JG: Lymphocyte sequestration through S1P lyase inhibition and disruption of S1P gradients. Science 2005, 309:1735–1739
28. Chiba K, Matsuyuki H, Maeda Y, Sugahara K: Role of sphingosine 1-phosphate receptor type 1 in lymphocyte egress from secondary lymphoid tissues and thymus. Cell Mol Immunol 2006, 3:11–19
29. Rosen H, Goetzl EJ: Sphingosine 1-phosphate and its receptors: an autocrine and paracrine network. Nat Rev Immunol 2005, 5:560–570
30. Schwab SR, Cyster JG: Finding a way out: lymphocyte egress from lymphoid organs. Nat Immunol 2007, 8:1295–1301
31. von Wenckstern H, Zimmermann K, Kleuser B: The role of the lysophospholipid sphingosine 1-phosphate in immune cell biology. Arch Immunol Ther Exp (Warsz) 2006, 54:239–251
32. Gräler MH, Huang MC, Watson S, Goetzl EJ: Immunological effects of transgenic constitutive expression of the type 1 sphingosine 1-phosphate receptor by mouse lymphocytes. J Immunol 2005, 174:1997–2003

33. Matloubian M, Lo CG, Cinamon G, Lesneski MJ, Xu Y, Brinkmann V, Allende ML, Proia RL, Cyster JG: Lymphocyte egress from thymus and peripheral lymphoid organs is dependent on S1P receptor 1. Nature 2004, 427:355–360
34. Wang W, Huang MC, Goetzl EJ: Type 1 sphingosine 1–phosphate G protein-coupled receptor (S1P1) mediation of enhanced IL-4 generation by CD4 T cells from S1P1 transgenic mice. J Immunol 2007, 178:4885–4890
35. Windh RT, Lee MJ, Hla T, An S, Barr AJ, Manning DR: Differential coupling of the sphingosine 1-phosphate receptors Edg-1, Edg-3, and H218/Edg-5 to the G(i), G(q), and G(12) families of heterotrimeric G proteins. J Biol Chem 1999, 274:27351–27358
36. Kim CH: Reining in FoxP3(+) regulatory T cells by the sphingosine 1-phosphate-S1P1 axis. Immunol Cell Biol 2009, 87:502–504
37. Kitagawa-Sakakida S, Schwartz RH: Multifactor cis-dominant negative regulation of IL-2 gene expression in anergized T cells. J Immunol 1996, 157:2328–2339
38. Powell JD, Lerner CG, Ewoldt GR, Schwartz RH: The -180 site of the IL-2 promoter is the target of CREB/CREM binding in T cell anergy. J Immunol 1999, 163:6631–6639
39. Sundstedt A, Sigvardsson M, Leanderson T, Hedlund G, Kalland T, Dohlsten M: In vivo anergized CD4+ T cells express perturbed AP-1 and NF-kappa B transcription factors. Proc Natl Acad Sci USA 1996, 93:979–984
40. Lopes JE, Torgerson TR, Schubert LA, Anover SD, Ocheltree EL, Ochs HD, Ziegler SF: Analysis of FOXP3 reveals multiple domains required for its function as a transcriptional repressor. J Immunol 2006, 177:3133–3142

Fas-Independent T-Cell Apoptosis by Dendritic Cells Controls Autoimmune Arthritis in MRL/*lpr* Mice

Takashi Izawa[1,2], Tomoyuki Kondo[1], Mie Kurosawa[1], Ritsuko Oura[1], Kazuma Matsumoto[2], Eiji Tanaka[2], Akiko Yamada[1], Rieko Arakaki[1], Yasusei Kudo[1], Yoshio Hayashi[1], Naozumi Ishimaru[1]*

1 Department of Oral Molecular Pathology, Institute of Health Biosciences, The University of Tokushima Graduate School, Tokushima, Japan, **2** Department of Orthodontics and Dentofacial Orthopedics, Institute of Health Biosciences, The University of Tokushima Graduate School, Tokushima, Japan

Abstract

Background: Although autoimmunity in MRL/*lpr* mice occurs due to a defect in Fas-mediated cell death of T cells, the role of Fas-independent apoptosis in pathogenesis has rarely been investigated. We have recently reported that receptor activator of nuclear factor (NF)-κB ligand (RANKL)-activated dendritic cells (DCs) play a key role in the pathogenesis of rheumatoid arthritis (RA) in MRL/*lpr* mice. We here attempted to establish a new therapeutic strategy with RANKL-activated DCs in RA by controlling apoptosis of peripheral T cells. Repeated transfer of RANKL-activated DCs into MRL/*lpr* mice was tested to determine whether this had a therapeutic effect on autoimmunity.

Methods and Finding: Cellular and molecular mechanisms of Fas-independent apoptosis of T cells induced by the DCs were investigated by *in vitro* and *in vivo* analyses. We demonstrated that repeated transfers of RANKL-activated DCs into MRL/*lpr* mice resulted in therapeutic effects on RA lesions and lymphoproliferation due to declines of $CD4^+$ T, B, and $CD4^-CD8^-$ double negative (DN) T cells. We also found that the Fas-independent T-cell apoptosis was induced by a direct interaction between tumor necrosis factor (TNF)-related apoptosis-inducing ligand-receptor 2 (TRAIL-R2) on T cells and TRAIL on Fas-deficient DCs in MRL/*lpr* mice.

Conclusion: These results strongly suggest that a novel Fas-independent apoptosis pathway in T cells maintains peripheral tolerance and thus controls autoimmunity in MRL/*lpr* mice.

Citation: Izawa T, Kondo T, Kurosawa M, Oura R, Matsumoto K, et al. (2012) Fas-Independent T-Cell Apoptosis by Dendritic Cells Controls Autoimmune Arthritis in MRL/*lpr* Mice. PLoS ONE 7(12): e48798. doi:10.1371/journal.pone.0048798

Editor: Pierre Bobé, Institut Jacques Monod, France

Received February 23, 2012; **Accepted** October 1, 2012; **Published** December 12, 2012

Funding: The study was supported by Funding Program for Next Generation World-Leading Researchers in Japan (LS090) and a Grant-in-Aid for Scientific Research from the Ministry of Education, Culture, Sports, Science and Technology of Japan (no. 21249090, no. 23390429, no. 23659879). The funders had no role in study design, data collection and analysis, decision to publish, or preparation of the manuscript.

Competing Interests: The authors have declared that no competing interests exist.

* E-mail: ishimaru@dent.tokushima-u.ac.jp

Introduction

Rheumatoid arthritis (RA) is an autoimmune disease characterized by chronic inflammation and synovial infiltration of immune cells [1]. Various immune cells are implicated in the pathogenesis of RA in patients and in murine models [2]. Furthermore, interactions between osteoclasts and immune cells, such as T-cell priming by activated dendritic cells (DCs), may contribute to the pathogenesis of RA in human and murine models [3].

DCs are professional antigen-presenting cells (APCs) that are present in low numbers in all body tissues [4]. Immature DCs are capable of antigen uptake. After activation via Toll like receptor triggering [5,6], RANK/RANKL [7], or CD40/CD40L signaling [8,9], DCs are activated as evidenced by an up-regulation of MHC molecules and costimulatory molecules, such as CD40, CD80, and CD86 [10]. These mature DCs are no longer capable of antigen uptake but are endowed with the capacity to initiate antigen-specific T-cell responses. In contrast, immature DCs are believed to induce antigen-specific tolerance via the induction of regulatory T cells or the deletion of antigen-specific T cells [11]. Thus, DCs play a pivotal role in orchestrating the immune response against self and non-self antigens. Although several studies have demonstrated that DCs control autoimmunity in several diseases, including in RA [12,13], it remains unclear how DCs regulate autoreactive T cells in the periphery.

We recently reported that crosstalk between Fas and receptor activator of NF-κB ligand (RANKL) maintains peripheral DCs associated with autoimmunity [14]. RANKL, a type II membrane protein of tumor necrosis factor (TNF) family, is expressed on osteoblasts, stromal cells, and activated T cells, and binds to the signaling receptor RANK and decoy receptor osteoprotegerin [7,15–18]. RANK is widely expressed in the myelomonocytic lineage, ranging from osteoclast precursors to mature DCs [15,19]. Mice lacking RANKL or RANK display severely reduced osteoclastogenesis, show defects in early differentiation of T and B cells, lack lymph nodes (LNs), and fail to develop mammary glands [20,21]. Although we demonstrated that activation of Fas-deficient DCs was up-regulated by engagement of RANKL signaling, and that the single transfer of RANKL-stimulated DCs resulted in accelerated autoimmune arthritis in MRL/*lpr* mice [14], we speculated whether repeated transfers, but not single

transfer, of RANKL-stimulated DCs modify peripheral tolerance and control autoimmunity in MRL/*lpr* mice.

In this study, we investigated the precise molecular mechanism of the interaction between activated DCs and T cells in the autoimmune response of MRL/*lpr* mice. Furthermore, a proposed new DC therapy was tested to see if it would regulate RA lesions in MRL/*lpr* mice.

Results

Therapeutic effect of repeated transfers of DCs on RA lesions in MRL/*lpr* mice

We have previously demonstrated that a single injection of RANKL and type II collagen (CII)-stimulated bone marrow-derived dendritic cells (BMDCs) into MRL/*lpr* mice resulted in elevated severity of RA lesions through up-regulation of T-cell functions including T-helper (Th)1-typed cytokine production or proliferative response [14]. We have also reported that the phenotype of the increased DC from MRL/*lpr* mice was myeloid DC showing $CD11b^+$ $CD11c^+$ $CD8\alpha^-$ [14]. Therefore, we hypothesized that multiple interactions of activated DCs with peripheral T cells can control autoimmunity. Thus we tried to analyze the regulatory mechanism of autoimmunity in MRL/*lpr* mice by multiple transfers of activated DCs. To elucidate how activated DCs regulate autoreactive T cells in the periphery, we performed repeated transfer experiments with RANKL and CII-activated DCs into MRL/*lpr* mice. As shown in Figure 1A, BMDCs from MRL/*lpr* or MRL/+/+ mice were stimulated with RANKL and CII, and subcutaneously transferred into MRL/*lpr* mice three times during a week from 4 to 5 weeks of age. At 16 weeks after the transfers, all the organs of the recipient MRL/*lpr* mice were analyzed. Pathological findings of RA lesions in non-treated MRL/*lpr* mice (20 weeks of age) showed subsynovial mononuclear inflammatory infiltrate, erosion and destruction of articular cartilage by panus, fibrosis, and synovial proliferation (Figure 1 B). Histological analysis showed that RA lesions from RANKL and CII-stimulated MRL/*lpr* DC- (*lpr* DC-) transferred mice were clearly improved although a slight infiltration of mononuclear cells was observed in the subsynovial connective tissue of the treated mice (Figure 1B). In contrast, there was not a significant effect of +/+ DC transfer on the RA lesion compared with that of *lpr* DC-transferred mice (Figure 1B). Histological evaluation revealed that the arthritic score of lesions from *lpr* DC-transferred mice was significantly lower than that from the control mice (Figure 1C). In addition, we compared RA lesions between RANKL-stimulated DCs- and RANKL+CII-stimulated DCs-transferred recipients. There was more therapeutic effect on RA lesions by multiple transfers of RANKL+CII-stimulated DCs than that of RANKL-stimulated DCs (Figure S1A). Furthermore, the levels of rheumatoid factor (RF) (IgM and IgG) in the sera of *lpr* DC-transferred mice were significantly reduced compared with those from controls (Figure 1D). Anti-double strand (ds)DNA and anti-CII Abs, but not anti-nuclear antibody (ANA), as well as RF in the recipients transferred with activated *lpr* DCs were significantly reduced compared with those in the recipients transferred with control DCs (Figure S1B). It is still unclear whether antibody against CII influences the induction of RA lesions in MRL/*lpr* mice. It has been reported that severe RA lesions can develop without anti-CII antidoby [22,23]. However, it is possible that CII-primed DCs enhance *in vivo* immune reaction including CII-specific response in MRL/*lpr* mice. On the other hand, when *lpr* DCs stimulated without CII antigen were transferred into *lpr* recipients, autoantidoby production of the sera from the recipients was not changed (Figure S1C). Therefore, the antigen-specific response plays a key role in triggering the immunoregulatory mechanism in the recipient mice. When we compared a single transfer and multiple transfers (three times) of activated *lpr* DCs into MRL/*lpr* mice, there was a clear difference for severity of autoimmune lesions between these two treatments (Figure 1E and 1F). These results showed that repeated transfers of activated DCs could control RA lesions in MRL/*lpr* mice. In particular, *lpr* DCs activated with both RANKL and CII could regulate the RA lesion effectively.

Effect of repeated transfers of activated DCs on lymphoproliferation in MRL/*lpr* mice

It is well known that splenomegaly and systemic lymphoadenopathy are observed in MRL/*lpr* mice [24–26]. The size of the spleen and inguinal lymph nodes (ILNs) from *lpr* DC-transferred mice was smaller than those from control mice (Figure 2A). The total cell number of spleen and ILNs in *lpr* DC-transferred mice was also significantly decreased compared with that of control mice (Figure 2B). Furthermore, to clarify which subset of lymphocytes was reduced in the spleen and ILNs from *lpr* DC-transferred mice, the T cell subpopulation was analyzed by flow cytometry. The number of $CD4^+$ T cells from the spleen and ILNs of *lpr* DC-transferred mice was significantly decreased compared with that of control mice (Figure 2C). In contrast, no difference was observed in the number of $CD8^+$ T cells of the spleen and ILNs between *lpr* DC-transferred mice and control mice (Figure 2C). Moreover, the number of $B220^+Thy1.2^-$ B cells of spleen and ILNs from *lpr* DC-transferred mice was significantly reduced compared with that from control mice (Figure 2D). In addition, a significantly decreased number of $CD4^-CD8^-$ double negative (DN) T cells of ILNs, not spleen, in RANKL+CII-*lpr* DC-transferred mice was found (Figure 2E). Next we attempted to determine the T and B cell apoptosis and maturation *in vivo*. As we could not detect apoptosis of the cells at 8 or 12 weeks after the transfer, we analyzed apoptosis of T and B cells at 2 weeks after the transfer. Flow cytometric analysis showed that annexin-V^+ $CD4^+$ T, B, and DNT cells of ILNs from *lpr* DCs-transferred recipients were significantly increased compared with those from +/+ DCs-transferred recipients (Figure S2A, B, C, D). In addition, there were no differences in the frequency of memory ($CD44^{high}$ $CD62L^-$) $CD4^+$ T cells between *lpr* and +/+ DCs-transferred recipients although $CD44^{high}$ $CD62L^+$ activated $CD4^+$ T cells of *lpr* DC-transferred mice were relatively increased compared with that of controls (Figure S3A). As to B cell maturation markers (CD27 and CD5), there were no differences between three groups (Figure S3B). Those findings suggest that repeated interactions between Fas-deficient DCs and T cells regulate $CD4^+$ T-cell activation. Additionally, the repeated transfers of DCs controlled B and $CD4^-$ $CD8^-$ DNT cell survival in the periphery and reduced lymphoproliferation as well as RA lesions in MRL/*lpr* mice.

On the other hand, when carboxyfluorescein succinimidyl ester (CFSE)-labeled +/+ or *lpr* DCs were subcutaneously injected into MRL/*lpr* mice, significantly increased $CFSE^+$ $CD11c^+$ *lpr* DCs were observed compared with those from MRL+/+ mice in ILNs at 2 weeks after the transfer (Figure S4A). Therefore, *in vivo* experiment shows that the survival of *lpr* DCs may be better than that of +/+ DCs. Moreover, we detected increased $CFSE^+CD11c^+$ cells in spleen as well as ILNs from *lpr* DC-transferred mice comparing with +/+ DC-transferred mice (Figure S4B). It is possible that a therapy using normal DCs may be effective for RA lesions by any manipulation for longer survival.

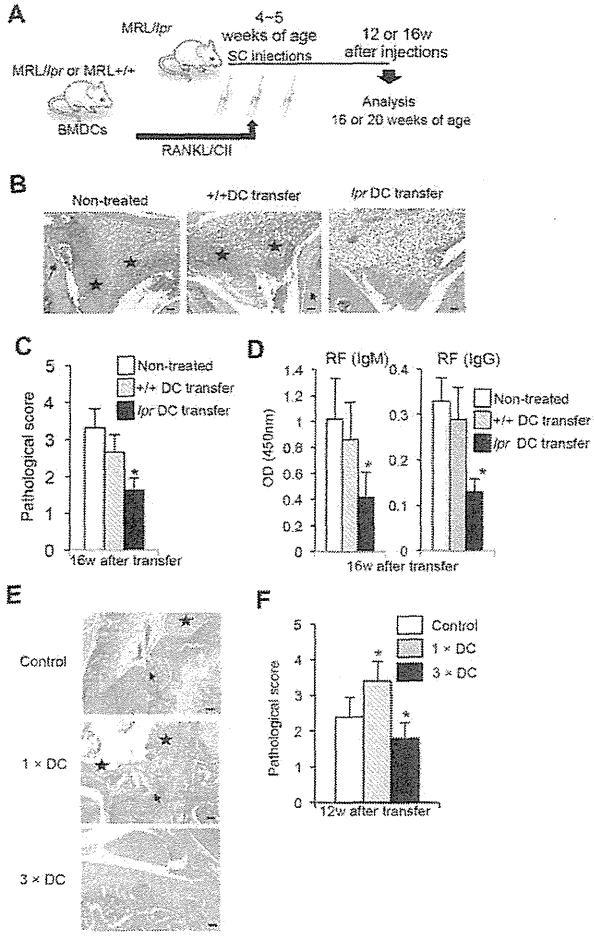

Figure 1. Therapeutic effect of repeated transfers of DCs on autoimmune arthritis. (A) Experimental protocol is shown. BMDCs from female MRL+/+ and MRL/*lpr* mice were stimulated with RANKL and CII, and then female MRL/*lpr* mice received a total of 3 injections of the BMDCs every other day distributed over 6 day period. At 16 weeks after transfer (20 weeks of age), the recipient MRL/*lpr* mice were analyzed. (B) Histology of joint from recipient mice. Histological photos with HE staining are shown as representative of the recipient mice at 16 weeks after transfers. Arrow; bone erosion or synovial proliferation, star; mononuclear inflammatory infiltrate, fibrosis, or panus. Scale bar: 100 μm (n = 7, 10 and 12 per group respectively). (C) The histological score of the recipient mice was evaluated at 16 weeks after repeated transfers. Data are shown as means ± SD. (n = 7, 10 and 12 per group respectively). (D) Rheumatoid factor (RF) (IgM and IgG) antibody was measured by ELISA. Values are shown as means ± SD (n = 7, 10 and 12 per group respectively). OD = optical density. (E) RA lesions of control, a single DC transferred (1× DC), and multiple DC transferred (3× DC) MRL/*lpr* mice were compared. Histological photos with HE staining are shown as representative of the recipient mice at 12 weeks after transfers. Scale bar: 100 μm (n = 5 per group respectively). (F) The histological score of the recipient mice was evaluated at 12 weeks after repeated transfers. Data are shown as means ± SD (n = 5 per group respectively). *$p<0.05$.
doi:10.1371/journal.pone.0048798.g001

T-cell functions in DC-transferred mice

We next evaluated T-cell functions of *lpr* DC-transferred mice at 12 weeks after the transfer. Purified $CD4^+$ T cells from ILNs of recipient MRL/*lpr* mice were stimulated with plate-coated anti-CD3 monoclonal antibody (mAb) (0–0.5 μg/ml) and-CD28 mAb (10 μg/ml) for 72 hours to analyze proliferation with the incorporation of [^{3}H]-Thymidine. T-cell response in ILNs from *lpr* DC-transferred MRL/*lpr* mice was significantly decreased compared with that form +/+ DC-transferred and control mice (Figure 3A). By contrast, when T cells from the recipient MRL+/+ mice transferred with multiple transfers of activated DCs were analyzed, there was no change in the proliferation of $CD4^+$ T cells between three groups (Figure S5). Moreover, cytokine productions using the culture supernatants from anti-CD3 mAb-engaged $CD4^+$ T cells of spleen and ILNs were analyzed by ELISA. Th1-typed cytokine production such as IL-2 and IFN-γ from *lpr* DC-transferred MRL/*lpr* mice was significantly lower than that from +/+ DC-transferred and control mice (Figure 3B). By contrast, IL-10 production in the ILN $CD4^+$ T cells from *lpr* DC-transferred MRL/*lpr* mice was significantly enhanced compared with that from +/+ DC-transferred recipients (Figure 3B). By repeated transfer of the DCs, the immune environment displaying Th1 cytokine profile of $CD4^+$ T cells was shifted to Th2 cytokine profile including IL-10. It was possible that the induction of IL-10-dependent tolerogenic environment by multiple DC transfers might play a crucial role in the progression of autoimmunity in MRL/*lpr* mice. As for IL-4 and IL-17 production, there was no significant difference between *lpr* DC-transferred and control mice (Figure 3B). These results indicate that activated DCs crucially regulate the peripheral T-cell functions in MRL/*lpr* mice. Activated and CII-exposed *lpr* DC may be capable of controlling T-cell survival in the periphery by continuing the stimulation. As for signal II initiated by CD28 ligation on T cells, the results of T-cell functions suggest that the T cell signaling controlled by signal I, II, and III may be imbalanced in the DC-transferred recipient mice. Therefore, if normal DCs can survive to continue stimulating T cells like activated *lpr* DCs, it is possible that normal DCs might induce the same effect with the imbalance of T cell signaling. In addition, we performed the flow cytometric analysis of thymic T cells (CD4 and CD8) of the treated recipient mice (Figure S6A). There was no change between the treated and control mice. Therefore, multiple transfers of DCs could not influence T cell differentiation in the thymus. Moreover, we analyzed regulatory T (T_{reg}) cells of ILNs and spleen in the recipient MRL/*lpr* mice treated with multiple transfers of DCs. There was no difference in the frequency of $CD25^+$ $Foxp3^+$ $CD4^+$ T_{reg} cell of ILNs and spleen between +/+ DCs- and *lpr* DCs-transferred recipients (Figure S6B).

T-cell apoptosis induced by activated DCs

Repeated DC transfers reduced the cell number of $CD4^+$ T cells in MRL/*lpr* mice. However, it remained unclear whether apoptosis of $CD4^+$ T cells could be induced by repeated interactions with DCs. Thus, T cells of ILNs from MRL/*lpr* mice were repeatedly (three times) co-cultured with RANKL and CII-stimulated BMDCs from MRL/*lpr* or MRL+/+ mice (Figure 4A). Although the *in vivo* immune response in the recipient treated with multiple transfer was not clear, *in vitro* repeated interactions of activated DCs with T cells could be one of clues to understand the *in vivo* immune response. In brief, T cells were repeatedly transferred into each well in which T cells were co-cultured with RANKL and CII-stimulated-*lpr* or +/+ DCs for 24 hours. After the third incubation, apoptotic cells expressing annexin-V were detected by flow cytometry. Apoptosis of $CD4^+$, but not $CD8^+$, T cells co-cultured with *lpr* DCs was significantly increased compared with those incubated with +/+ DCs (Figure 4B). In addition, when compared the mean fluorescence intensity (MFI) of annexin-V on the co-cultured $CD4^+$ T cells, the MFI on $CD4^+$ T cells co-cultured with RANKL and CII-stimulated *lpr* DCs was

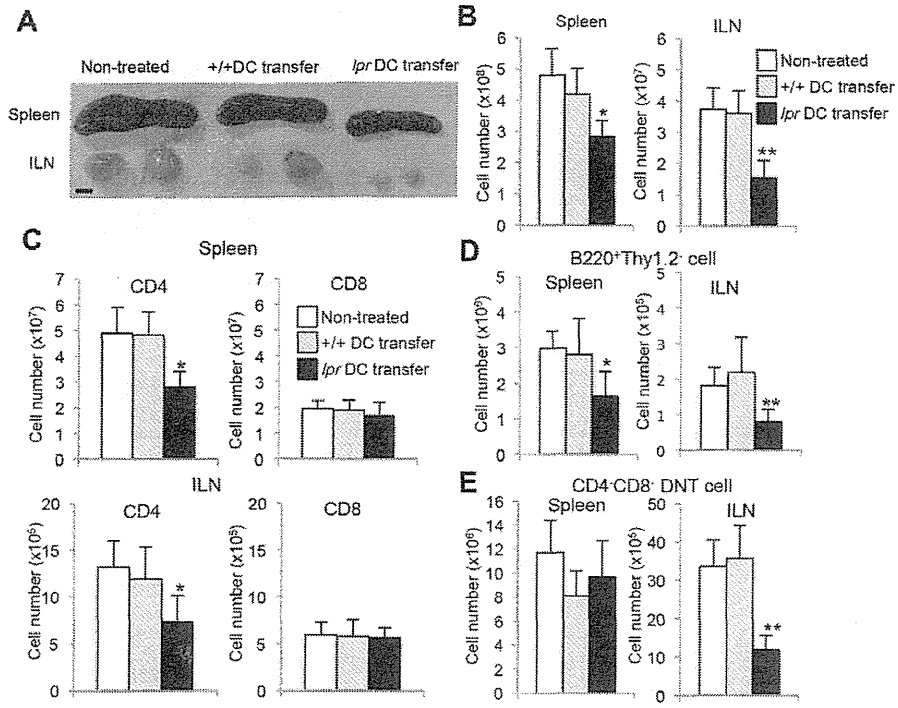

Figure 2. Reduced lymphoproliferation of MRL/*lpr* mice following repeated transfers of DCs. (A) Spleen and ILNs from the recipient mice are shown. Photos are representative of the recipient mice (16 weeks of age) at 12 weeks after the transfer. Values are shown as means ± SD (n = 5, 7 and 7 per group respectively). (B) The total cell number in the spleen, and ILNs is shown. Scale bar: 5 mm. (C) T cell numbers in the spleen and ILNs of the recipient mice. Flow cytometry was performed using spleen and ILN cells. The number of $CD4^+$ and $CD8^+$ T cells is shown. (D) B cell ($B220^+$ $Thy1.2^-$) number in the spleen and ILNs of the recipient mice. (E) $CD4^-$ $CD8^-$ $CD3^+$ DNT cell number in the spleen and ILNs of the recipient mice. Values are shown as means ± SD (n = 5, 7, and 7 respectively per group). *$p<0.05$, **$p<0.005$.
doi:10.1371/journal.pone.0048798.g002

significantly increased in contrast to that with RANKL and CII-stimulated +/+ DCs (Figure 4C). The $CD4^+$ T-cell apoptosis was induced by *lpr* DCs dependent on the number of DCs (Figure 4B). In contrast, apoptosis of $CD8^+$ T cells was not enhanced by repeated co-culturing with *lpr* DCs (Figure 4B). There was no increased apoptosis of DNT cells *in vitro* by repeated interactions with DCs (Figure 4D). In addition, apoptosis of $B220^+$ $Thy1.2^-$ B cells from MRL/*lpr* and MRL+/+ mice was not induced by the repeated co-culture with *lpr* DCs (Figure 4D). We confirmed that the number of living and dead cells before the co-culture with T cells was not changed after the co-culture for 24 hours. While it is possible that *lpr* $CD4^+$ T cells may control DNT cells and B cells in the periphery directly or indirectly, there may be still veiled *in vivo* mechanism of the survival of abnormal DNT cells. As for the cultured BMDCs, we prepared the same number between +/+ and *lpr* DCs (Figure 4). When ovalbumin (OVA) or bovine serum albumin (BSA), and RANKL-stimulated *lpr* DCs were repeatedly co-cultured with $CD4^+$ T cells from MRL/*lpr* mice, there was no significant increase of apoptotic cells in contrast to the co-culture with CII and RANKL-stimulated *lpr* DCs (Figure 4E). Additionally, we performed the *in vitro* experiment using $CD4^+$ T cells from MRL+/+ mice. When $CD4^+$ T cells from MRL+/+ mice were co-cultured repeatedly with RANKL+CII-stimulated *lpr* DCs, a significant increase of +/+ $CD4^+$ T cell apoptosis like *lpr* $CD4^+$ T cells was not observed (Figure 4F). These results suggest that Fas-independent T-cell apoptosis is induced by repeated interactions of activated DCs. However, the precise mechanism of *in vivo* immune response in the recipient treated with multiple transfer has not been clear.

Molecular mechanism of Fas-independent T-cell apoptosis

To elucidate the molecular mechanism responsible for Fas-independent T-cell apoptosis, we compared the gene expression of RANKL/CII-*lpr* DC-stimulated *lpr* $CD4^+$ T cells with RANKL/CII-+/+ DC-stimulated *lpr* $CD4^+$ T cells using a PCR-based SuperArray method focusing on apoptosis-related genes. Of the 96 genes analyzed, the most increased gene was TRAF3 (>3-fold), and 10 genes including TNFSF10b (TRAIL-R2), and caspase 8 showed >2-fold increase compared with +/+ DC-stimulated $CD4^+$ T cells (Figure 5A). It has been reported that TRAIL-R plays an important role in activation-induced apoptosis of $CD4^+$ T cells [27]. Therefore, we hypothesized that Fas-independent apoptosis of $CD4^+$ T cells is induced by the interaction between TRAIL-R2 on $CD4^+$ T cells and TRAIL on activated DCs in MRL/*lpr* mice. To confirm the result of the PCR-array, mRNAs of the up-regulated genes were evaluated by quantitative RT-PCR. Consistent with the data from the RCR-array, mRNAs of TRAF3, TRAIL-R2, and caspase 8 of T cells stimulated with *lpr* DCs were significantly increased compared with those from control T cells (Figure 5B). In contrast, the anti-apoptotic gene Bcl-2 was significantly decreased (Figure 5B). Next, we examined TRAIL expression on RANKL-stimulated DCs from MRL/*lpr* mice. Although a previous report demonstrated that TRAIL expression on DCs was up-regulated by IFN-γ stimulation [28], it

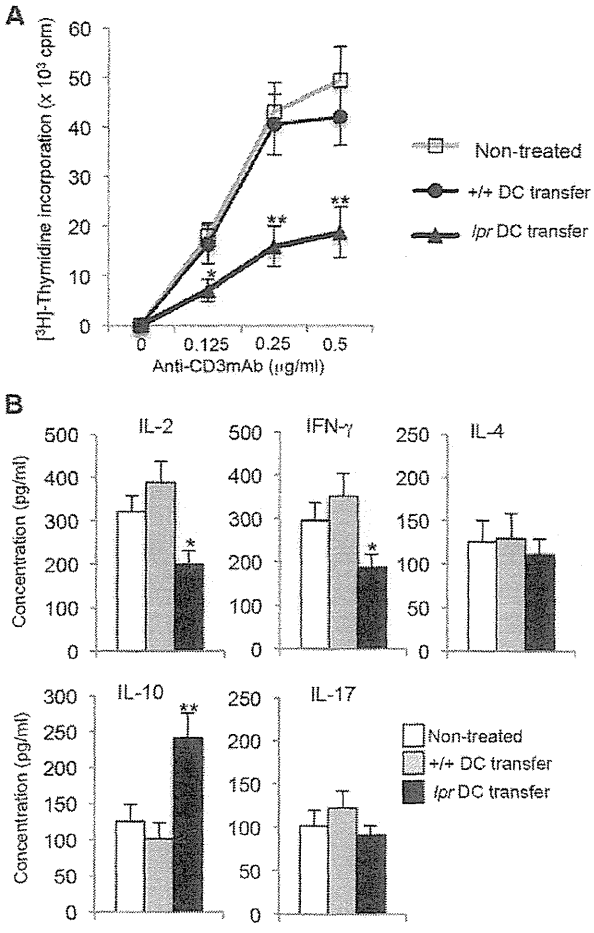

Figure 3. T cell responses in DC-transferred MRL/*lpr* mice. (A) Proliferative responses of ILN $CD4^+$ T cells from the recipients and control mice were analyzed. Purified $CD4^+$ T cells were stimulated with plate-coated CD3 mAb (0–0.5 μg/ml) and CD28 mAb (10 μg/ml) for 72 hours. The proliferative response was evaluated by $[^3H]$ thymidine incorporation. Values are means ± SD (n = 4, 5, and 5 respectively per group). Results are representative of three independent experiments with similar results. (B) The culture supernatants for 24 h (anti-CD3 mAb: 0.5 μg/ml; anti-CD28 mAb: 10 μg/ml) as described above were analyzed for cytokine productions including IL-2, IFN-γ, IL-4, IL-10, and IL-17 by ELISA. Values are means ± SD (n = 4, 5, and 5 respectively per group). *p<0.05, **p<0.005.
doi:10.1371/journal.pone.0048798.g003

was unclear whether TRAIL on DCs can be controlled by the RANK/RANKL signal. In our study, TRAIL expression on DCs from MRL/*lpr* mice was significantly enhanced by RANKL stimulation (Figure 5C). No difference was observed in the increased expression of *lpr*DCs and +/+ DCs induced by IFN-γ stimulation (Figure 5C). Moreover, we performed an additional experiment using anti-TRAIL mAb to block *in vitro* T cell apoptosis by multiple interactions with activated DCs. An anti-TRAIL mAb could inhibit *in vitro lpr* T-cell apoptosis by the interactions with activated *lpr* DCs (Figure 5D). These results suggest that Fas-independent T-cell apoptosis is induced by a direct interaction between TRAIL-R on T cells and TRAIL on DCs. This shows that apoptosis of Fas-deficient $CD4^+$ T cells may be controlled through TRAIL/TRAIL-R. Therefore, although normal T cells are resistant to TRAIL/TRAIL-R-mediated apoptosis as described in the previous report [29], the maintenance of peripheral T cells in human patients with abnormal Fas/FasL system may be regulated by the TRAIL/TRAIL-R-mediated pathway.

TRAIL/TRAIL-R2-mediated apoptosis of Fas-deficient $CD4^+$ T cells

To further confirm TRAIL/TRAIL-R2-mediated apoptosis of Fas-deficient $CD4^+$ T cells by RANKL+CII-stimulated DCs, we examined whether siRNA for TRAIL gene silencing inhibits T-cell apoptosis. BMDCs from MRL/*lpr* mice were treated with TRAIL gene-specific siRNA, and then stimulated with RANKL and CII for 48 hours. During the last 24 hours of the culture, purified $CD4^+$ T cells from MRL/*lpr* mice were repeatedly (three times) co-cultured with the DCs for 8 hours. Apoptotic cells (annexin-V^+PI^+) were analyzed by flow cytometry as shown in Figure 6A. When the effect of the TRAIL gene-specific siRNA on the surface expression of DCs from MRL/*lpr* mice was evaluated, up-regulated TRAIL expression on RANKL+CII-stimulated DCs was seen to decrease in a dose-dependent manner, indicating that the knockdown was effective (Figure S7A, B). By contrast, the increased level of TRAIL in stimulated DCs was unchanged by treatment with control siRNA (Figure S7A, B). Interestingly, apoptosis of $CD4^+$ T cells induced by repeated co-culturing with RANKL and CII-stimulated DCs was significantly reduced by treatment with TRAIL siRNA although there was no change in T-cell apoptosis following co-culturing with control siRNA-treated DCs (Figure 6B, C). Furthermore, we assessed the repeated transfer using TRAIL siRNA-treated DCs. BMDCs from MRL/*lpr* mice were treated with TRAIL siRNA *in vitro*, and then repeatedly transferred into MRL/*lpr* mice during 4 to 5 weeks of age. At 12 weeks (16 weeks of age) after the transfers, autoantibody production of serum in the recipients such as RF was measured by ELISA. Although serum titer of RF in the recipient MRL/*lpr* mice transferred with control siRNA-treated DCs were significantly decreased compared with untreated MRL/*lpr* mice at 4, 8, and 12 weeks after the transfers, RF titer of the MRL/*lpr* recipients transferred with TRAIL siRNA-treated DCs was not reduced, and was equal to that of control MRL/*lpr* mice (Figure 6D). In addition to RF, we analyzed anti-dsDNA and anti-CII Abs. We could detect a significant increase of anti-dsDNA and anti-CII Abs in the recipient transferred with TRAIL siRNA-treated DCs compared with that with control siRNA-treated DCs (Figure S8). Moreover, histological analysis showed that the therapeutic effect of repeated transfers of DCs on RA lesions was inhibited by *in vitro* treatment with TRAIL siRNA for DCs (Figure 6E). This result indicates that activated DCs expressing TRAIL plays a key role in regulating Fas-independent apoptosis of peripheral T cells.

Discussion

DCs are crucial for the initiation of T-cell immunity and play an important role in the onset and regulation of immune responses in RA [13,30]. Our previous report demonstrated that a single transfer of RANKL-stimulated DCs resulted in the exacerbation of RA lesions in MRL/*lpr* mice [14]. In contrast, the present study revealed the therapeutic effect of repeated transfers of DCs on the RA lesions and lymphoproliferation in MRL/*lpr* mice. In terms of recent therapeutic strategies for RA, modulation of several cytokines, such as TNF-α, IL-1, and IL-6 are therapeutic targets in RA [2,31]. However, since cytokines regulate a broad range of inflammatory processes and since this regulatory network is considerably complicated in the pathogenesis of RA, the clinical application of such therapies is risky because of potential side

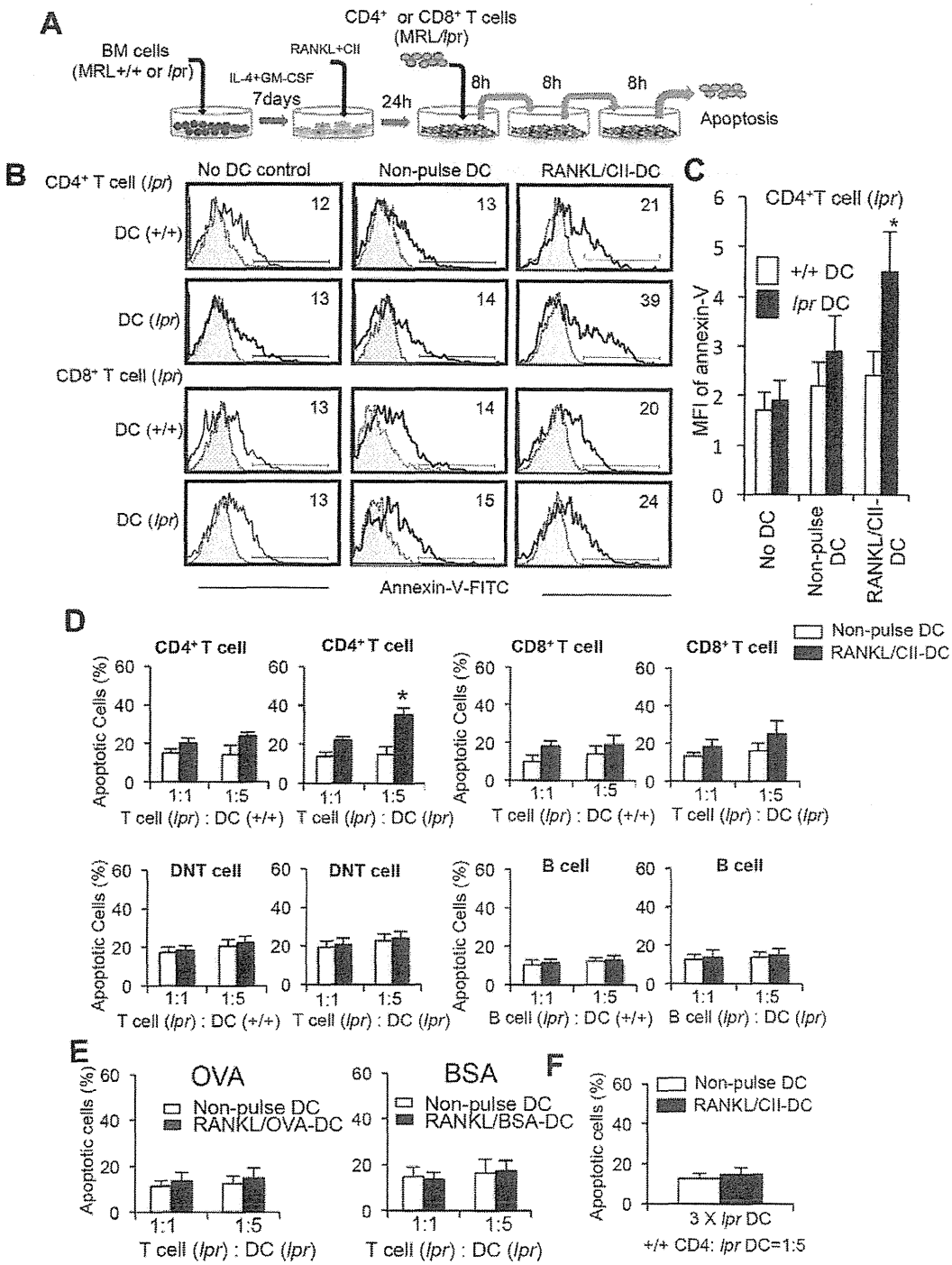

Figure 4. Fas-independent T-cell apoptosis in DC-transferred MRL/*lpr* mice. (A) Experimental protocol of T cell apoptosis by repeated co-culture with DCs. Total T cells from MRL/*lpr* mice (5×10^4) were repeatedly (three times) co-cultured with BMDCs (2.5×10^5) from MRL+/+ or MRL/*lpr* mice for 8 hours without interval. BMDCs were stimulated with RANKL and CII for 24 hours before the co-culturing. (B) After the third co-culture, apoptosis of $CD4^+$ and $CD8^+$ T cells expressing annexin-V was detected by flow cytometry. Staining of T cell with FITC-labeled isotype control Ab is shown as a dotted line. Results are shown as representative of three independent experiments with similar results. (C) MFI of annexin-V on $CD4^+$ T cells was calculated, and the data are shown as the means ± SD of triplicate samples. (D) Induction of T-cell apoptosis by repeated co-culturing with activated DCs. Purified $CD4^+$, $CD8^+$, DNT, and $B220^+$ cells (5×10^4) were repeatedly co-cultured with BMDCs (5 and 25×10^4). Annexin-V^+ cells are shown as the means ± SD of triplicate samples. The experiments were repeated three times with similar results. *$p<0.05$. (E) BMDCs were stimulated with RANKL and, OVA or BSA (10 μg/ml) for 24 hours before the co-culturing. Purified $CD4^+$ cells (5×10^4) were repeatedly co-cultured with BMDCs (5 and 25×10^4). Annexin-V^+ cells are shown as the means ± SD of triplicate samples. The experiments were repeated three times with similar results. (F)

Purified $CD4^+$ cells (5×10^4) from ILNs in MRL+/+ mice were repeatedly co-cultured with *lpr* BMDCs (25×10^4). Annexin-V^+ cells are shown as the means ± SD of triplicate samples. The experiments were repeated three times with similar results.
doi:10.1371/journal.pone.0048798.g004

effects on the immune system. In this study, no changes were observed in any other organs in recipient mice that were subjected to repeated transfers of DCs when all the organs were histopathologically examined. It has been reported that repeated injections of DCs matured with TNF-α induces antigen-specific protection against experimental autoimmune encephalomyelitis

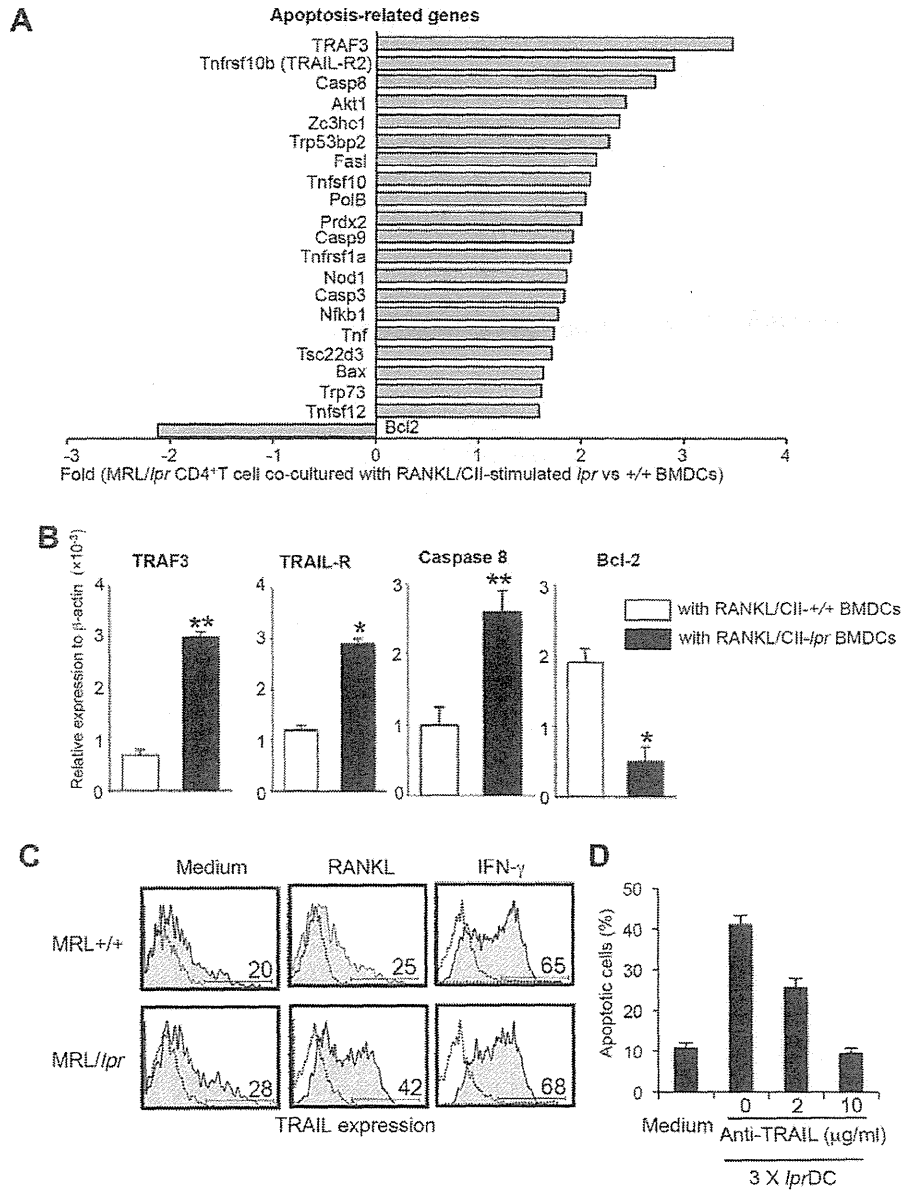

Figure 5. T-cell apoptosis via TRAIL/TRAIL-R2. (A) Real-time RT-PCR for a wide array of apoptosis-related genes was performed using mRNA samples of MRL/*lpr* $CD4^+$ T cells repeatedly stimulated with MRL/*lpr* and MRL+/+ BMDCs. Gene expression of $CD4^+$ T cells repeatedly stimulated with MRL/*lpr* BMDCs was compared with those stimulated with MRL+/+ BMDCs (controls). Genes with increased and decreased expression are shown as fold of control. The experiments were repeated twice with similar results. (B) The mRNA expression of TRAF3, TRAIL-R2, caspase 8, and Bcl-2 was confirmed by quantitative real-time PCR analysis. Relative expression to β-actin level is shown as means ± SD from triplicate samples. The experiments were repeated three times with similar results. (C) Up-regulation of TRAIL expression on MRL/*lpr* BMDCs by RANKL was detected by flow cytometry. Staining of DC with FITC-labeled isotype control Ab is shown as a dotted line. The experiments were repeated three times with similar results. (D) *lpr* CD4+ T cells were repeatedly co-cultured with activated *lpr* DCs in the presence of anti-TRAIL mAb. Data are shown as means ± SD of triplicate samples. *$p<0.05$, **$p<0.005$.
doi:10.1371/journal.pone.0048798.g005

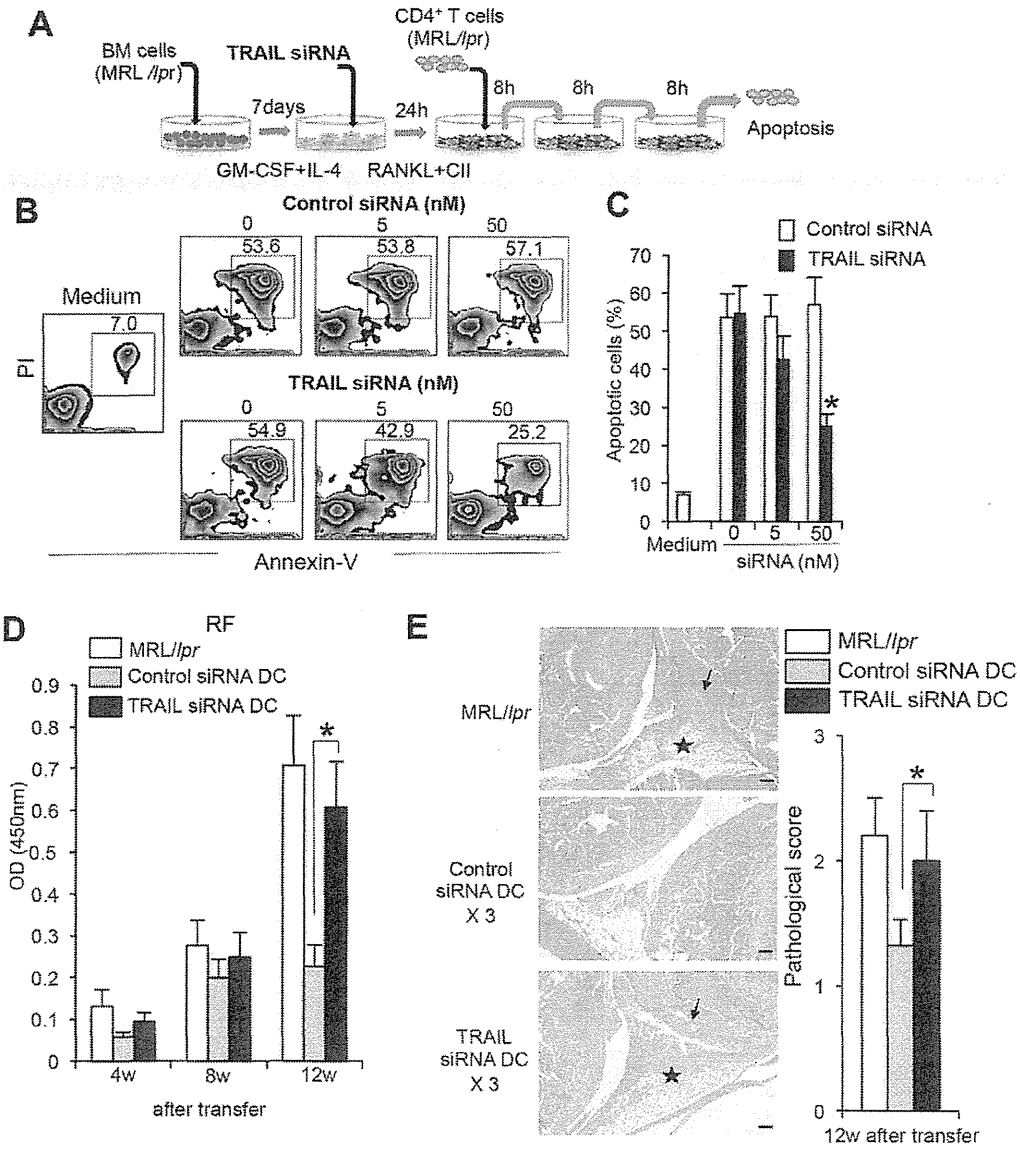

Figure 6. Regulation of Fas-independent T cell apoptosis by TRAIL siRNA-treated DCs. (A) BMDCs from MRL/*lpr* mice were treated with TRAIL gene-specific siRNA or control siRNA for 24 hours, and then stimulated with RANKL and CII for 48 hours. Purified $CD4^+$ T cells of LNs from MRL/*lpr* mice were repeatedly (three times) co-cultured with the activated DCs for 8 hours by transfer into each new well. (B) Expression of TRAIL on activated BMDCs treated with TRAIL siRNA or control siRNA was analyzed by flow cytometry. Results are representative of two independent experiments with similar results. (C) Apoptosis of $CD4^+$ T cells cocultured with siRNA-treated DCs was analyzed by flow cytometry with Annexin-V and PI. Results are representative of two independent experiments. (D) Apoptotic cells (%) are shown as the mean ± SD from triplicate samples. The experiments were repeated three times with similar results. (E) *In vitro* TRAIL siRNA-treated and control DCs were injected three times into MRL/*lpr* mice (4 weeks of age). After 12 weeks after the transfers, RF level of sera from the recipient mice (16 weeks of age) was detected by ELISA. Values are means ± SD. (n = 5). The experiments were repeated twice with similar results. (F) Histology of joint from recipient mice. Histological photos with HE staining are shown as representative of five mice in each group at 12 weeks after transfers. Arrow; bone erosion or synovial proliferation, star; mononuclear inflammatory infiltrate, fibrosis, or panus. Scale bar: 100 μm. Histological score is shown as means ± SD. (n = 5) *$p<0.05$.
doi:10.1371/journal.pone.0048798.g006

(EAE) in mice [32]. Although it was reported that overexpression of IL-10 is associated with the manifestations of ALPS and SLE, the reduced Th2 cell population producing IL-10 is related to the disease severity in RA [33–36]. In our study, since *lpr* DC therapy was effective for RA lesions, but not renal lesions, there might be different effects of DC transfer on autoimmune lesions in each target organ. Regarding antigen-specificity in our model, RANKL-stimulated DCs were incubated with CII antigen *in vitro* in this study and in our previous report. Without CII antigen incubation, the significant effects of DC transfer on autoimmunity were not fully observed. Although we have not clarified "antigen specificity" using only CII antigen, *in vitro* experiment using OVA or BSA antigen implies that CII antigen may play a important role in triggering the onset of autoimmunity of MRL/*lpr* mice.

Therefore, DC therapy with CII antigen in addition to potent stimulation by RANKL can be more effective for autoimmunity.

We transferred the DCs into MRL/*lpr* at 4 weeks of age in which lymphadenopathy and splenomegaly based on lymphproliferation of the mice was not observed. By the multiple transfers of DCs, $CD4^+$ T cells might be killed directly by *lpr* DCs while it is possible that apoptosis of DNT cell and B cells might be indirectly induced. According to our preliminary experiment, multiple transfers of DCs at 10 weeks of age could not be effective for suppression of RA lesion and lymphadenopathy of MRL/*lpr* mice. In this study, it is suggested that beneficial of the multiple transfers of activated DCs is confined to the *lpr* background and antigen-specific immune response.

Our previous report demonstrated that crosstalk between RANKL and Fas signaling in DCs controls autoimmune arthritis in MRL/*lpr* mice [14]. Moreover, it was reported that RANKL regulates Fas expression and Fas-mediated apoptosis in osteoclast [37]. To determine whether such control of autoimmunity by DCs could be used as a therapeutic strategy, repeated transfers of activated DCs were performed in this study to see if there could prevent autoimmune arthritis in MRL/*lpr* mice. We found that TRAIL expression on BMDCs from MRL/*lpr* mice was up-regulated by RANKL stimulation. TRAIL is known to interact with at least two death receptors, including death receptor 4 (DR4, TRAIL-R4) and death receptor 5 (DR5, TRAIL-R5), and two decoy receptors (decoy receptor 1 [DcR1, TRAIL-R3, TRID] and decoy receptor 2 [DcR2, TRAIL-R4, TRUNDD]) [38–40]. Apoptosis through TRAIL/TRAIL-R has been reported in several tumor cell lines [38]. The apoptosis is mediated by DR4 and DR5, which possess intracellular death domains similar to those of TNF receptor I and Fas [38,41]. In addition, death domains of TRAIL-R activate mitochondria-dependent and mitochondria-independent pathways of apoptosis through FADD-caspase 8, leading to activation of the caspase cascade [42–44]. A previous report described that TRAIL-overexpressed DCs could inhibit the development of CII-induced arthritis (CIA) [45]. Although the precise molecular mechanism is obscure, it is possible that RANKL-induced TRAIL expression on DCs from MRL/*lpr* mice triggers T cell apoptosis. Abnormal system of Fas/FasL is not found in all other models and in all human RA. Autoimmunity is known to be caused by multi-factors, and is a complex disease. RA lesions in MRL/*lpr* mice resembling human RA are the most common among RA animal models. Therefore, the abnormality of Fas/FasL system in immune cells is considered to influence the pathogenesis of human RA. Fas-deficient DCs might be more useful than normal DCs expressing Fas molecule for treatment of autoimmunity in our study. The fact that Fas-deficient DCs become more activated than normal DCs could affect Fas-independent T cell apoptosis to prevent autoimmunity in MRL/*lpr* mice. This suggests that DC therapy might be helpful for autoimmunity of patients with abnormal Fas expression on the immune cells, and that a therapy for autoimmunity using normal DCs might fail to prevent or treat autoimmune diseases. Although it is still difficult to apply a new DC therapy for human RA, any therapeutic strategy with controlling autoreactive T cells by DCs will be useful in the feature. In addition, although the effect observed in our study is confined to MRL/*lpr* mice, the mice are the most common and useful for understanding the pathogenesis of autoimmune RA. Therefore, any unique phenomenon or effect using MRL/*lpr* mice will pave to a road to define the mechanism of autoimmunity and develop any new therapy for autoimmunity.

Cell death of peripheral T cells is one of the systems used to maintain immunological tolerance [46]. Fas/FasL in T cell apoptosis plays a crucial role in the maintenance of peripheral tolerance [46]. Although the relationship between apoptosis of peripheral T cells and TRAIL/TRAIL-R2 is unclear, it has been reported that mice deficient in TRAIL have a severe defect in thymocyte apoptosis and that TRAIL is important in the induction of autoimmune diseases [47,48]. TRAIL/TRAIL-R-mediated T-cell apoptosis may be promoted in a Fas-deficient situation by an interaction with DCs that highly express TRAIL. In contrast, it has also been reported that reciprocal expression of TRAIL and FasL in T helper 1 and 2 cells plays a key role in T-cell apoptosis in T helper subset differentiation [27]. Our results suggest that activated Fas-deficient T cells expressing TRAIL-R is induced by repeated interactions with TRAIL-expressing DCs. It is possible that TRAIL/TRAIL-R-mediated apoptosis of T cells plays a key role in an alternative of apoptosis pathway.

In summary, repeated transfers of activated Fas-deficient DCs resulted in a therapeutic effect on lymphoproliferation and autoimmune arthritis in MRL/*lpr* mice due to Fas-independent apoptosis of $CD4^+$ T cells through TRAIL/TRAIL-R2. Our new therapeutic approach using this alternative apoptosis pathway could prove to be a powerful strategy for the prevention and cure of immune disorders in the near future.

Materials and Methods

Ethics

This study was conducted according the principles expressed in the Declaration of Helsinki. The study was approved by the Institutional Review Board of the University of Tokushima (toku09021).

Mice

MRL/*Mp-lpr/lpr* mice (MRL/*lpr*: aged 4–12 weeks; n = 75) and MRL+/+ mice (aged 4–12 weeks; n = 50) were purchased from Japan SLC (Shizuoka, Japan). All mice were maintained under specific pathogen-free conditions at our animal facility. We analyzed female mice at 16 or 20 weeks of age.

Bone marrow-derived DCs (BMDCs)

BMDCs were generated from the bone marrow of MRL/*lpr* or MRL+/+ mice as described previously [49]. BMDCs were stimulated with 100 ng/mL RANKL and 50 μg/mL chicken type II collagen (CII) for 48 hours. 2×10^6 BMDCs/a mouse were transferred three times or once into recipient MRL/*lpr* mice at the base of the tail by subcutaneous injections in 200 μL PBS at the age of 4 weeks.

Histopathology

All organs were taken from the mice, fixed with 4% phosphate-buffered formaldehyde (pH 7.2), and prepared for histological examination. The sections (4 μm in thickness) were stained with hematoxylin and eosin (HE). Histological grading of inflammatory arthritis was performed according to the methods of Edwards *et al* [42]. as follows: a 1-point score indicates hyperplasia/hypertrophy of synovial cells, fibrosis/fibroplasia, proliferation of cartilage and bone, destruction of cartilage and bone, and mononuclear cell infiltrate. We have confirmed that any inflammatory findings are observed in over 90% MRL/*lpr* mice at 16 or 20 weeks of age. In approximately 20% female MRL/*lpr* mice at 12 weeks of age, any slight findings such as hyperplasia of synovial cells and mononuclear cell infiltration were observed. These findings of arthritis lesions in MRL/*lpr* mice are consistent with those in previously demonstrated reports [50–53].